

**Performance, Throughput Properties, and Optimal Location  
Evaluation for Max-pressure Control**

A THESIS

SUBMITTED TO THE FACULTY OF THE GRADUATE SCHOOL  
OF THE UNIVERSITY OF MINNESOTA

BY

**Simanta Barman**

IN PARTIAL FULFILLMENT OF THE REQUIREMENTS  
FOR THE DEGREE OF  
MASTER OF SCIENCE

Advised by Dr. Michael W. Levin

November, 2022

Copyright  
by  
Simanta Barman  
2022

*To my grandparents.*

## Acknowledgements

I would like to extend my sincerest gratitude to Dr. Levin for motivating me to do good research, introducing me to different topics and nudging me in the right direction when I got stuck. I remember feeling hopeful and inspired after every individual meeting I had with him. The completion of this Thesis would not be possible without his guidance.

## Abstract

Max pressure (MP) signal timing is an actuated decentralized signal control policy. Rigorous mathematical studies have proven stability or bounded total vehicle queues over a long period for all feasible demands. Those studies also established the theoretical benefits of different MP policies. However, the theoretical studies make some assumptions about traffic properties that may not represent reality, the effects of which are not explored much in the literature under realistic traffic conditions. The first portion of this study focuses on examining how different variations of MP control perform in realistic scenarios and finding the most practical policy among those for implementation in real roads. Microsimulation models of seven intersections from two corridors, County Road (CR) 30 and CR 109 from Hennepin County, Minnesota were created. Real life demand and current signal timing data provided by Hennepin County, Minnesota were used to make the simulations as close to reality as possible. Then, the performance comparisons of current actuated-coordinated (AC) signal control with an acyclic MP and two variations of cyclic MP policies are shown. The performance of different control policies in terms of delay, throughput, worst lane delay and number of phase changes are also presented. How different parameters affect performance of the MP policies is also presented. We found that better performance can be achieved with cyclic max pressure policy by allowing phase skipping when no vehicles are waiting. Findings from this study also suggest that most of the claimed performance benefits can still be achieved in real life traffic conditions even with the simplified assumptions made in the theoretical models. In most cases, MP control policies outperformed current signal control.

The second portion of this study covers deployment strategies of MP control under limited budget and the associated stability properties. According to

the theoretical results published so far, it can stabilize a network if all intersections are equipped with MP control for all stabilizable demands. However, budget constraints may not allow the installation of MP control on all intersections. Previous work did not consider a limited number of MP controlled intersections while proving the stability properties. Therefore, it is not clear whether a network can still be stabilized with a limited deployment of MP control. Using Lyapunov drift techniques, this thesis proves that even with a limited deployment, MP control can stabilize a network within feasible demand. Then, an optimization formulation to find the optimal intersections to install MP control given a limited budget is presented. We also present an efficient greedy algorithm to solve that optimization problem and prove that the algorithm solves the problem to optimality. Numerical results from simulations conducted on the downtown Austin network using an in-house custom simulator called AVDTA are then presented. The change in theoretical maximum servable demands for different amounts of deployments obtained from the optimization problem seemed to mostly match with simulation results. We found that limited deployment of MP control almost always performed better than random deployment of MP control in terms of servable stable demand. Average total queue length and link density were observed to decrease as the number of MP controls increased, which indicates better network performance. Average travel times per vehicle also decreased with installations of MP controls, which shows how the travelers would benefit from more MP controls.

# Contents

<b>1</b>	<b>Introduction</b>	<b>1</b>
1.1	Background . . . . .	1
1.2	Problem Statement . . . . .	3
1.3	Contributions . . . . .	5
1.4	Outline . . . . .	6
<b>2</b>	<b>Literature review</b>	<b>9</b>
<b>3</b>	<b>Modified MP Controls</b>	<b>15</b>
3.1	Notation and Terminology . . . . .	16
3.2	Max pressure controls . . . . .	17
3.2.1	Acyclic Max-pressure Control . . . . .	18
3.2.2	Cyclic Max-pressure Control . . . . .	18
3.3	Simulation Settings . . . . .	20
3.4	Simulation Results . . . . .	23
3.4.1	Impact of Max-pressure Parameters . . . . .	23
3.4.1.1	Impact on Delay . . . . .	24
3.4.1.2	Impact on Throughput . . . . .	26
3.4.2	Performance using Best Parameters . . . . .	30
3.4.2.1	Delay . . . . .	30

3.4.2.2	Throughput . . . . .	34
3.4.2.3	Worst Lane Delay . . . . .	35
3.4.2.4	Phase Changes . . . . .	38
<b>4</b>	<b>Limited Deployment of MP Control</b>	<b>41</b>
4.1	Notation and Terminology . . . . .	42
4.2	Limited Deployment . . . . .	45
4.2.1	Stable region for limited deployment . . . . .	47
4.2.2	Stability with limited deployment . . . . .	48
4.3	Limited Deployment Formulation . . . . .	57
4.3.1	Demand Maximization Under Limited Budget . . . . .	57
4.3.2	Demand Maximization According to Origin to Destination Proportions under Limited Budget . . . . .	59
4.4	Numerical Results . . . . .	61
<b>5</b>	<b>Conclusions</b>	<b>71</b>
5.1	Performance Evaluation of Modified Cyclic MP in Simulation . . . . .	71
5.2	Throughput Properties and Optimal Intersections . . . . .	73
5.3	Limitations and Recommendations . . . . .	74

# List of Figures

- 3.1 Intersections along CR 30 and CR 109 corridors. . . . . 21
- 3.2 Average delay (in seconds) per vehicle per hour at the intersections along the CR 30 corridor during different demand periods. 27
- 3.3 Average delay (in seconds) per vehicle per hour at the intersections along the CR 109 corridor during different demand periods. 28
- 3.4 Effect of MP timesteps on average delay using AMP during different demand periods. . . . . 29
- 3.5 Throughput per hour at the intersections along the CR 30 corridor during different demand periods. . . . . 31
- 3.6 Throughput per hour at the intersections along the CR 109 corridor during different demand periods. . . . . 32
- 3.7 Average delays (in seconds) per vehicle per hour at intersections along CR 30 and CR 109. . . . . 33
- 3.8 Throughput per hour at intersections along CR 30 and CR 109. . 36
- 3.9 Percent change in worst lane’s total delay per hour from AC signal controllers by max-pressure controllers along CR 30 and CR 109 corridors. . . . . 37
- 3.10 Number of phase changes per hour at the intersections along CR 30 and CR 109 under different demand periods. . . . . 39

4.1	Downtown Austin network, red nodes are MP controlled and other nodes are controlled using timings from Austin network data. . . . .	63
4.2	Stability detection by binary search for different deployments of MP control (Data from only 1 repetition of MC is plotted.) . . .	64
4.3	Maximum stable demands achieved with different deployment policies of MP nodes. . . . .	66
4.4	Maximum stable demands achieved with different deployment policies of MP nodes. . . . .	67
4.5	Change in different performance metrics with increase in limited deployment. . . . .	68

# List of Tables

3.1	Level of service for County Road 30 corridor. . . . .	22
3.2	Controller's implemented in this thesis. . . . .	22



# Chapter 1

## Introduction

### 1.1 Background

Traffic signal controllers play an important role in dealing with traffic congestion. Well-planned traffic signal control have shown to improve system performance significantly (Lioris et al., 2016a; Levin and Boyles, 2017; Sun and Yin, 2018). Current traffic signals in intersections use predefined timing to actuate phases based on historical demand for a certain period of a day. Demands may fluctuate in different periods of the day due to many reasons. Therefore, using the same signal timing for all demands does not result in optimal phase timings. That is why an adaptive traffic signal controller is more desirable which can react to the changes in demand while controlling the signal activation. Among the traffic signal controllers developed so far, the only one with theoretical maximum throughput guarantees is called max-pressure (MP) control. The concept of MP control was introduced independently by Varaiya (2013) and Wongpiromsarn et al. (2012) in the context of traffic signal control.

MP control is a maximally stable, adaptive traffic signal control policy which

activates phases based on real time traffic data. A controller is stable for a network if over a large period of time the sum of the queues of vehicles is bounded for a feasible demand. Moreover, a controller is maximally stable for a network if the controller can stabilize all possible stabilizable demands. Here the feasible demands is the set of all demands that can be served by some other controller including the theoretical controllers. Therefore, the maximum stability property implies that the maximally stable control can serve all demands that can be theoretically served. Previous studies have rigorously proven MP control to be maximally stable under certain assumptions.

It is also a decentralized policy which means that unlike centralized signal control policies which require a large amount of information from the network, MP control only requires traffic information from the adjacent links to an intersection. This makes MP control computationally efficient which allows it to scale very well for large networks. MP control selects a phase with the objective of maximizing throughput which results in implicit signal coordination by the flow of traffic. Current signal timing is specific to each period, whereas the max-pressure control is a general algorithm that applies the same to all periods. These properties make MP control very attractive to implement in real life.

The analytical benefits of max-pressure control have been established through rigorous proofs in previous work including Varaiya (2013) and Xiao et al. (2014). However, the queueing models in the analytical studies made assumptions about the traffic flow that differ from reality. Varaiya (2013) used a store and forward queueing model similar to Vickrey (1963)'s bottleneck or point queue model. According to point queue model links are uncongestible, have infinite capacity, are always traveled at freeflow speed, the queues are represented by a single point that occupies no physical space at the downstream end of links and congestion is localized as link interaction is ignored as stated by Zhang et al. (2013). Lim-

itations of point queues motivated the use of Gawron (1998)'s spatial queue model in Xiao et al. (2014) which represents a more realistic link model where maximum queue lengths are enforced which allows considering realistic traffic phenomena like queue spillback. However, spatial queues only consider one congested physical section at the downstream end of a link where in reality a link can have multiple congested and uncongested sections throughout the link. Also, spatial queues assume that all vehicles in a queue move together without considering the effects of delays of individual vehicles. The theoretical models created using these queueing models require validation under realistic traffic conditions.

## 1.2 Problem Statement

Analytical results proving maximum throughput from MP control unfortunately does not guarantee any level of improvement over current signals since maximum throughput could also be achieved by fixed signal timings. It is also not clear how max-pressure control affects intersection delay, besides maintaining a stable value of delay whenever possible. Consequently, advancing the implementation of max-pressure control in practice requires a demonstration of the benefits compared to current signal timing. Not much work has been done to test these theoretical results in simulation with real-world traffic data. Sun and Yin (2018) showed that non-cyclic MP performed better than cyclic MP and actuated signal controls and provided a new modified MP with minimum green time. However, they used an actuated signal control logic provided in the Ring Barrier Control module of Vissim which does not replicate real-world control and also, they used only a single peak period's scaled traffic demand. This thesis uses real world traffic control with real-life traffic demands from different periods of the day.

The use of acyclic MP control like Varaiya (2013)'s MP control is also a

problem for practical use as it does not ensure a maximum waiting time for each phase. Therefore, vehicles may end up waiting for a very long time before the phase that allows them to move activates. Acyclic phase selection of MP control also seems random and confusing to drivers. Le et al. (2015) proposed a cyclic MP control with nonzero amount of time allocated to each phase. However, if green times of a phase is not sufficiently long to allow vehicle movement then actuating that phase becomes less useful. Also, having to specify a fixed cycle length which is a requirement for that MP control is a weakness. Levin et al. (2020) provided a modified cyclic MP control with proof of stability which addresses these issues. In this thesis we tweak the that modified cyclic MP control to make it perform slightly better and then compare simulation results to determine the best control policy to implement in real life.

Several papers have already presented numerical results (Levin and Boyles, 2017; Sun and Yin, 2018; Barman and Levin, 2022) indicating MP control performs better compared to other signal controllers. However, all of the papers so far used MP on all of the signalized intersections. Even though it would be ideal to install MP in all the intersections according to those results, it may not be feasible due to budget constraints. Budget and other installation constraints may only allow installing MP in some intersections. However, it is not clear how installing MP on some intersections would affect performance of the traffic network. Even though MP is proven to be maximally stable when all intersections have MP control, no stability guarantee exists in the literature when MP is installed on only some of the intersections. Along with nonexistent theoretical guarantees previous works do not consider a limited deployment of MP control in simulations either. This thesis tries to deal with this exact problem. For maximum stability for limited deployment of MP control on  $n$  intersections we only consider the feasible demands obtained by improving the control on those

$n$  intersections. This means that we consider all the demand that the network can serve with any other controller installed on those  $n$  intersections while analyzing maximum stability. However, this feasible region may be smaller than the feasible region where all the intersection's control are modifiable. Can MP control still achieve maximum stability if it is used only on some of the intersections? How would the performance of the system be affected? These are some of the questions this thesis tries to address. This thesis also determines the optimal intersections to install MP control. The optimal order of installation is also determined which allows more MP control to be installed in the future as more budget becomes available. Being able to determine the best intersections given the budget and the order of installation of MP control provides practical engineering and planning advantages.

### 1.3 Contributions

We compare Varaiya (2013)'s acyclic MP control, Levin et al. (2020)'s cyclic MP control with and without phase skipping, and currently active AC signal controls' performance under different real-life traffic demands in microsimulation. Intersection demand (including turning movement counts) and baseline pretimed signals are from data collected by Hennepin County for those intersections at different demand periods throughout the day. This is the first study evaluating conventional MP control against professional pretimed signals using actual traffic data. We compare the different signal controller's performance based on several metrics like delay, throughput, worst lane delay, number of phase changes etc. to determine whether MP control can produce the claimed theoretical benefits over current AC signal controllers under realistic traffic conditions.

The other part of the contributions of this thesis are the following: we prove

that MP control achieves maximum stability even for a limited number of deployed MP controllers. We then present a mixed-integer-linear-programming (MILP) formulation to determine the optimal intersections for MP control installation. A greedy algorithm is also proposed and shown to be able to solve the MILP efficiently to optimality. Numerical results validating the theoretical results are then presented for the downtown Austin network.

## 1.4 Outline

The remainder of this thesis is organized as follows.

- Chapter 2 reviews the literature on MP control: how it has been used so far and what gaps in the literature still exists.
- Chapter 3 consists of the performance evaluation in simulation of different versions of MP control. The first section in that chapter presents the mathematical definitions of the different max-pressure controls. Description of the test network, demand data and current AC control are also presented. After that simulation settings are discussed briefly. Then, performance comparisons of the different signal controls from the simulations are presented.
- Chapter 4 deals with the throughput properties and optimal location selection for the limited deployment of MP controls. The first section in that Chapter redefines the mathematical notations used. Then, the limited deployment policy is introduced mathematically and a proof of stability for that policy is provided. An MILP formulation to find the intersections where MP control should be deployed is provided in the next section along with a greedy solution algorithm. After that numerical results from the theory and simulations are provided.

- Chapter 5 describes the conclusions of the study along with some of the limitations and recommendations for future studies on the topic.



## Chapter 2

# Literature review

Tassiulas and Ephremides (1992) first developed a maximum stability control for a queueing network with interdependent servers. They also presented an algorithm called backpressure (BP) or max-pressure to control the dependency among the servers by activating a subset of the servers so that the network remains maximally stable. Varaiya (2013) and Wongpiromsarn et al. (2012) independently presented this algorithm in the context of traffic networks and proved that traffic networks can also be maximally stabilized using this control. The implications of their results include: 1. Most importantly, the network throughput would be maximized, 2. The traffic signals can be controlled in a decentralized manner, 3. The only historical data required is the turn proportions which can be estimated (Varaiya, 2013; Gregoire et al., 2014a).

Gregoire et al. (2014b) showed that backpressure controller for traffic network from previous studies Varaiya (2013); Wongpiromsarn et al. (2012) resulted in loss of work conservation or transfer of traffic because of downstream congestion. They proposed a new traffic controller based on the backpressure algorithm that considers queue capacities to compute normalized pressure for

phases to decrease blocking or queue spillback probability. They showed that their capacity-aware backpressure policy outperformed previous backpressure policies Varaiya (2013); Wongpiromsarn et al. (2012) for high demand in simulation using a grid network with generated demands. Gregoire et al. (2014a) developed a new backpressure traffic signal control that does not require routing rates and showed the simulation results using the control on a  $21 \times 21$  grid network. Their conclusions based on the simulation results was that the algorithm tends to stabilize a significant part of the capacity region and benefits of their algorithm originated more from the realistic assumptions on queue measurements. However, they did qualify that even though the control algorithm can stabilize traffic networks with demand in a certain demand region, according to the simulations it is still not the optimal control. Sha and Chow (2019) found that a centralized control based on store and forward queueing model with the objective to minimize global network queues by adjusting green splits outperforms MP control. However, with increasing awareness of the traffic condition the drivers reroute and this causes the difference between the performance from the centralized control and MP control to decrease.

Varaiya (2013) and Gregoire et al. (2014a) assumed a store and forward queueing model with infinite queue capacity for the stability proofs. Other research has been conducted to make the assumptions more realistic. To handle noises in queue measurements Xiao et al. (2015a,b) developed extensions to the MP control with the proof of stability. Wu et al. (2018) gave a delay based MP control with the proof of stability. To model traffic queues more accurately Xiao et al. (2014) used spatial queue link model with finite traffic queues for their stability proof and Gregoire et al. (2014b) used spatial queue link model for their analysis. Li and Jabari (2019) later used kinematic wave theory to get an even more accurate traffic model which produced favourable results. Hao and

Yang (2019) presented a new hierarchical multigranularity traffic network with an extended MP control which outperformed fixed signal timing and acyclic MP control.

Several papers presented simulation results that showed that under different conditions, variations of MP control outperformed other traffic signal controls. Lioris et al. (2016b) presented MP control as efficacious arterial traffic regulator, Gregoire et al. (2014a) presented MP control with unknown routing, Kouvelas et al. (2014); Sun and Yin (2018) and Ramadhan et al. (2020) presented different versions of MP controller’s performance in simulation. Some papers presented capacity-aware (Gregoire et al., 2014b), utilization-aware (Chang et al., 2020), double pressure based (Yu et al., 2021), route choice included (Smith et al., 2019) versions of MP control that showed positive results. Some real experimental studies (Mercader et al., 2020; Dixit et al., 2020) also reported favourable results from different variations of MP control.

Lioris et al. (2016b) compared max-pressure control with and without adaptive routing to AC signal controller in realistic settings in simulation. Kouvelas et al. (2014) presented simulation results from two different max-pressure controls using an event-based simulator with variable simulation step that validated theoretical results. They also suggested further studies should be done to determine the optimal frequency for max-pressure calls for different networks during various demand periods. Levin and Boyles (2017) compared several intersection control policies, total system travel time and average travel time per vehicle were found to be the lowest for BP or MP control policy. Using travel times instead of queue lengths for calculating phase pressures, Mercader et al. (2020) showed that real life applicability of max-pressure controllers can be improved without loss of performance in simulation and results from a real-life intersection. The improvement in applicability comes from using travel times instead

of queue lengths which are harder to determine. Li et al. (2021a) proposed a BP control with estimated queue (BP-EQ) lengths to study the performance of BP control with inaccurate queue lengths for partially connected environment. They compared the simulation results of the performance using BP-EQ control with several penetration rates of connected vehicles and BP control with perfect knowledge about queue length with commercial adaptive controller at an isolated intersection and optimized fixed timing controller for a network. Simulation results showed performance increase for the BP controllers.

Recently, MP control have been used in the literature with technologies like connected and autonomous vehicles (CAV), autonomous intersection management (AIM), vehicle to infrastructure (V2I) and vehicle to vehicle (V2V) communications etc. Li et al. (2021a) showed the performance of MP or BP control at different levels of CAV penetration rates. Chen et al. (2020) analyzed AIM with pedestrians and gave a proof of stability. Levin et al. (2019) gave an MP control with AIM and dynamic lane reversal capable controller with proof of stability and showed significant performance improvement compared to first-come-first-served control. Rey and Levin (2019) developed a new traffic network control policy based on max-pressure algorithm for CAV's and they also gave a proof of stability. Yen et al. (2018) compared the fairness and vulnerabilities against cyber-attacks of four different BP based controllers.

The max-pressure or back-pressure controllers discussed in this chapter up to here are all acyclic, meaning they do not have to activate phases in a sequence. However, cyclic signal controllers are preferred in practice because it ensures that each phase will get activated at least once during a cycle and acyclic phase changes may confuse drivers Levin et al. (2020). Le et al. (2015) gave a cyclic max-pressure controller with proof of stability and showed positive results in simulation in terms of link density and average travel times. Pumar et al. (2015)

provide a cyclic extension to max-pressure control with performance gains observed in simulation results. Anderson et al. (2018) alter the max-pressure formulation to a cyclic max-pressure controller which perform better than actuated signal controllers. All of these cyclic MP control papers contained proof of stability. These cyclic max-pressure controllers however require a predefined fixed cycle length which requires manual fine tuning based on predicted demand. Levin et al. (2020) gave a demand responsive cyclic max pressure formulation along with a proof of stability where the cycle lengths are adaptive to real time demand.

Sun and Yin (2018) performed simulation using realistic traffic data using Varaiya (2013)'s MP, Le et al. (2015)'s cyclic MP and a modified MP with minimum predefined green time. They showed performance comparison between the MP controllers and actuated control. However, they did not have access to real life traffic control logic which they ended up generating in VISSIM. This thesis uses real traffic demand data and currently used AC signal control logics to create realistic simulations to compare performance from several variants of max-pressure controller with current AC signal controllers.

Other papers also tried to solve problems related to connected and autonomous vehicles (CAV) (Rey and Levin, 2019; Cao et al., 2020; Zhang et al., 2020), autonomous intersection management (AIM) with pedestrians (Chen et al., 2020), AIM with dynamic lane reversal (Levin et al., 2019), cyber attacks on traffic signals (Yen et al., 2018), vehicle routing (Taale et al., 2015; Gregoire et al., 2016; Liu et al., 2018), public transit signal priority (Xu et al., 2022), maximum stability dispatching policy (Li et al., 2021b; Kang and Levin, 2021; Xu et al., 2021) using similar analysis and proof techniques.

All of the papers mentioned so far, used MP control on all of the signalized intersections. The literature does not contain any proof of stability or numer-

ical results with a limited deployment of MP control. The maximum servable demand may change with different number of MP controlled intersections. So, stability guarantees that work with all MP controlled intersections may not work for a limited number of MP controlled intersections. This is because not having MP control in some intersection can reduce the maximum servable demand of the network. This thesis is the first study that attempts to tackle this problem.

## Chapter 3

# Modified MP Controls

Previous studies have theoretically shown that both acyclic and cyclic MP control can maximize network throughput. However, simplifying assumptions about traffic queues were made in those studies. The simulation studies conducted so far did not use real signal timing data. It is important to analyze the performance of the different MP controls in simulation using realistic traffic data before installing them in real life. Moreover, the theoretical studies only describes the performance in terms of throughput and does not mention how network delays would be affected. Practical usage of MP control in real life also requires selecting the optimal parameters for the MP algorithm that maximizes performance. The theoretical studies do not provide specific details on how to choose those parameters.

In this chapter, we analyze whether the claimed theoretical benefits of MP control can really be achieved. We also compare current actuated signal controllers with MP controls to determine whether the current controllers should be replaced. We implement different versions of MP control in simulation. Then, we analyze the performance of two traffic networks under those MP controls and

current real signal timing. The current signal timing data were obtained from MnDOT and the simulations were created to be as close to reality as possible. We also analyze the performance of the different controls under different traffic demand scenarios.

The acyclic MP controls require a parameter called the MP timesteps which indicates the time interval between MP calls. During an MP call, the MP optimization problem selects the optimal phase for activation. The optimization problem will be described in detail in this chapter. The cyclic MP controls require an additional parameter called the maximum cycle length. All of the phases must be activated in a pre-specified order at least once during the maximum cycle length. In this chapter we also try to determine the best parameters to improve the performance of the network in terms of average delays. The goal of this chapter is to examine whether current signal controls should be replaced by some version of MP control based on the simulation results.

### 3.1 Notation and Terminology

Consider a network  $\mathcal{G} = (\mathcal{N}, \mathcal{A})$  with set of nodes,  $\mathcal{N} = \mathcal{N}_z \cup \mathcal{N}_j$  and set of directed links  $\mathcal{A} = \mathcal{A}_r \cup \mathcal{A}_i \cup \mathcal{A}_s$  for this chapter.  $\mathcal{N}_z$  are the zones through which exogenous demand enters the network,  $\mathcal{N}_j = \mathcal{N}_i \cup \mathcal{N}_c$  is the set of junction nodes,  $\mathcal{N}_i$  are the signalized intersections and  $\mathcal{N}_c$  are the other nodes that connects two internal links.  $\mathcal{A}_r$  and  $\mathcal{A}_s$  are the entry and exit links that connects a zone node to a junction node and junction node to a zone node respectively and  $\mathcal{A}_i$  is the set of all other internal links that connects junction nodes.

Considering discrete time, queue evolution is tracked using store and forward queueing model. A turning movement  $(i, j)$  is a pair of any incoming link  $i$  and outgoing link  $j$  connected by a junction node. Assume the number of vehicles waiting to make the move  $(i, j)$  with turn proportion  $r_{ij}$ , is the queue length

$x_{ij}$ . We assume that exogenous demand  $d_i(t)$  entering the network through link  $i \in \mathcal{A}_r$  is an independent and identically distributed random variable with mean  $\bar{d}_i$  and maximum value  $\tilde{d}_i$  (assuming zones' capacity is physically limited).

Queue evolution can be represented using the following model-

$$x_{ij}(t+1) = x_{ij}(t) - y_{ij}(t) + d_i(t)r_{ij}(t) \quad \forall i \in \mathcal{A}_r \quad (3.1)$$

$$x_{jk}(t+1) = x_{jk}(t) - y_{jk}(t) + \sum_{i \in I(j)} y_{ij}(t)r_{jk}(t) \quad \forall j \in \mathcal{A} \setminus \mathcal{A}_r \quad \forall k \in O(j) \quad (3.2)$$

$I(j)$  and  $O(j)$  are the sets of incoming and outgoing links of  $j$  respectively. The intersection flow  $y_{ij}(t)$  for the movement  $(i, j)$  at time  $t$  is defined by

$$y_{ij}(t) = \min \{ x_{ij}(t), s_{ij}(t)Q_{ij} [\Delta t^{\text{MP}} - L_{ij}(t)] \} \quad (3.3)$$

where  $s_{ij}(t) = 1$  if the move  $(i, j)$  is permitted by the active phase  $p(t)$  at time  $t$  at the intersection  $n$  which connects the links  $i$  and  $j$  otherwise, 0.  $Q_{ij}$  is the capacity of the turning movement  $(i, j)$  which is reduced by  $[\Delta t^{\text{MP}} - L_{ij}(t)]$  where  $L_{ij}(t)$  is the lost time at time  $t$  and max-pressure timestep is  $\Delta t^{\text{MP}}$ .  $L_{ij}(t) = 0$  if at time  $t$  max-pressure control selects the previous phase  $p(t) = p(t - \Delta t^{\text{MP}})$  to activate again, otherwise if a phase change is required  $p(t) \neq p(t - \Delta t^{\text{MP}})$  then  $L_{ij}(t) = Y_{p(t)} + R_{p(t)}$ . Yellow time  $Y_{p(t)}$  and red time  $R_{p(t)}$  for a phase  $p(t)$  are the same as those from current AC signal controls.

## 3.2 Max pressure controls

Max-pressure control defines a weight  $w_{ij}(t)$  for each turning movement  $(i, j)$  as,

$$w_{ij}(t) = x_{ij}(t) - \sum_{k \in O(j)} x_{jk}r_{jk}(t) \quad (3.4)$$

### 3.2.1 Acyclic Max-pressure Control

Varaiya (2013)'s acyclic max-pressure formulation (3.5) to select the optimal phase for each node  $n \in \mathcal{N}_i$  at each time step  $t \in \{1, \dots, T\}$  is as follows,

$$\max \sum_{(i,j) \in \mathcal{A}^2} Q_{ij} S_{ij}(t) w_{ij}(t) \quad (3.5a)$$

$$\text{s.t. } \sum_{p \in P_n} z_n^p(t) = 1 \quad (3.5b)$$

$$z_n^p(t) \in \{0, 1\} \quad (3.5c)$$

$$S_{ij}(t) = \xi_{ij}^p z_n^p(t) \quad \forall (i, j) \in \mathcal{A}^2 \quad (3.5d)$$

where  $\xi_{ij}^p(t) \in \{0, 1\}$  indicates whether phase  $p$  activates movement  $(i, j)$  at time  $t$  and  $P_n = \{p_1, \dots, |P_n|\}$  is the ordered set of phases that can be activated at node,  $n$ . Here, objective function (3.5a) maximizes the pressure of a phase. Equation (3.5b) only allows one phase to be selected and Equation (3.5c) indicates whether phase  $p$  at node  $n$  is active at time  $t$ . (3.5d) determines  $S_{ij}(t)$  which indicates whether the movement  $(i, j)$  can be activated based on the phase that can be activated. Varaiya (2013)'s acyclic max-pressure control will henceforth be referred to as AMP.

### 3.2.2 Cyclic Max-pressure Control

Levin et al. (2020) modified AMP and made it cyclic with adaptive cycle lengths with minimum green time for each phase. They provide the integer linear program (3.6) which is solved for each node,  $n \in \mathcal{N}_i$ . This program looks ahead to a planning horizon,  $\mathcal{T}$  and at time step  $t$  the integer program is solved on the

horizon  $t + \tau \in [t, t + \mathcal{T} - 1]$ . Then, the program is solved again at  $t + 1$ .

$$\max \frac{1}{\mathcal{T}} \sum_{\tau=0}^{\mathcal{T}-1} \sum_{(i,j) \in \mathcal{A}^2} s_{ij}(t + \tau) w_{ij}(t) Q_{ij} [1 - L_{ij}(t + \tau)] \quad (3.6a)$$

$$\text{s.t.} \quad \sum_{p \in P_n} z_n^p(t + \tau) = 1 \quad \forall \tau \in [0, \mathcal{T} - 1] \quad (3.6b)$$

$$\begin{aligned} z_n^p(t + \tau) &\leq z_n^p(t + \tau - 1) + z_n^{p-1}(t + \tau - 1) & \forall p \in P_n, \\ & \forall \tau \in [0, \mathcal{T} - 1] \end{aligned} \quad (3.6c)$$

$$\begin{aligned} L_{ij}(t) &= \tilde{L}_{ij} \sum_{p \in P_n} (z_n^p(t) - z_n^p(t + \tau)) & \forall (i, j) \in \mathcal{M}_n, \\ & \forall \tau \in [0, \mathcal{T} - 1] \end{aligned} \quad (3.6d)$$

$$\varphi_n(t + \tau) \leq \frac{1}{2} \left( z_n^{p_1}(t + \tau) + z_n^{|P_n|}(t + \tau - 1) \right) \quad \forall \tau \in [0, \mathcal{T} - 1] \quad (3.6e)$$

$$c_n(t + \tau) \geq c_n(t + \tau - 1) + 1 - M\varphi_n(t + \tau) \quad \forall \tau \in [0, \mathcal{T} - 1] \quad (3.6f)$$

$$c_n(t + \tau) \leq c_n(t + \tau - 1) + 1 + M\varphi_n(t + \tau) \quad \forall \tau \in [0, \mathcal{T} - 1] \quad (3.6g)$$

$$c_n(t + \tau) \geq 1 - M(1 - \varphi_n(t + \tau)) \quad \forall \tau \in [0, \mathcal{T} - 1] \quad (3.6h)$$

$$c_n(t + \tau) \leq 1 + M(1 - \varphi_n(t + \tau)) \quad \forall \tau \in [0, \mathcal{T} - 1] \quad (3.6i)$$

$$c_n(t + \tau) \leq C_n \quad \forall \tau \in [0, \mathcal{T} - 1] \quad (3.6j)$$

$$\begin{aligned} s_{ij}(t + \tau) &= \sum_{p \in P_n} z_n^p(t) \xi_{ij}^p & \forall (i, j) \in \mathcal{M}_n, \\ & \forall \tau \in [0, \mathcal{T} - 1] \end{aligned} \quad (3.6k)$$

$$\begin{aligned} z_n^p(t + \tau) &\in \{0, 1\} & \forall p \in P_n, \\ & \forall \tau \in [0, \mathcal{T} - 1] \end{aligned} \quad (3.6l)$$

$$\varphi_n(t + \tau) \in \{0, 1\} \quad \forall \tau \in [0, \mathcal{T} - 1] \quad (3.6m)$$

The objective function that finds the maximum pressure within the time horizon  $\mathcal{T}$  is shown by (3.6a). Constraint (3.6b) restricts the program to select only one phase. Constraint (3.6c) ensures cyclic phase selection: a phase can be activated at time  $t$  only when the same or the previous phase in the cycle was

active at the previous time step  $t-1$ . Constraint (3.6d) determines the lost time while making sure lost time is 0 if the phase is unchanged from the previous time step. Constraint (3.6e) determines whether cycle restarted and sets  $\varphi_n(t)$  to 1 only when the previous phase was the last phase  $|P_n|$  in the cycle and phase at  $t$  changed to the first phase  $p_1$  in the cycle. Constraints (3.6f)-(3.6i) keeps track of the of duration since the last cycle started denoted by  $c_n(t)$ . Constraint (3.6j) restricts the maximum cycle length to  $C_n$ . Constraint (3.6k) determines the movements a phase activates. Constraint (3.6l) indicates whether a phase  $p$  is active and constraint (3.6m) indicates that  $\varphi_n(t + \tau)$  is a binary variable.

In this thesis we test two versions of this cyclic max-pressure (CMP) controller, with and without phase skipping referred to as CMP-S and CMP-NS respectively. AMP and CMP-NS are implemented using the formulations (3.5) and (3.6) respectively. Detailed proofs of the maximum stability properties for AMP and CMP-NS are given by Varaiya (2013) and Levin et al. (2020). For the implementation of CMP-S we relax the constraint (3.6c). We track the queue length at each simulation timestep and if there are no more vehicles the current phase can move then we move on to the next phase in the queue of phases. If no vehicles are waiting for the next phase in queue we skip that phase and move to the next phase and repeat this process. This may require calling max-pressure more often. Phase skipping in the absence of vehicle queues will ensure the perception of cyclicity of the controller while increasing the feasible region. CMP-S also stops a phase as soon as there are no more vehicles waiting to use the current phase which increases the green time utilization.

### 3.3 Simulation Settings

Seven intersections comprising two corridors from Hennepin County, MN were selected for closer study in simulation. Figure 3.1 shows the four and three

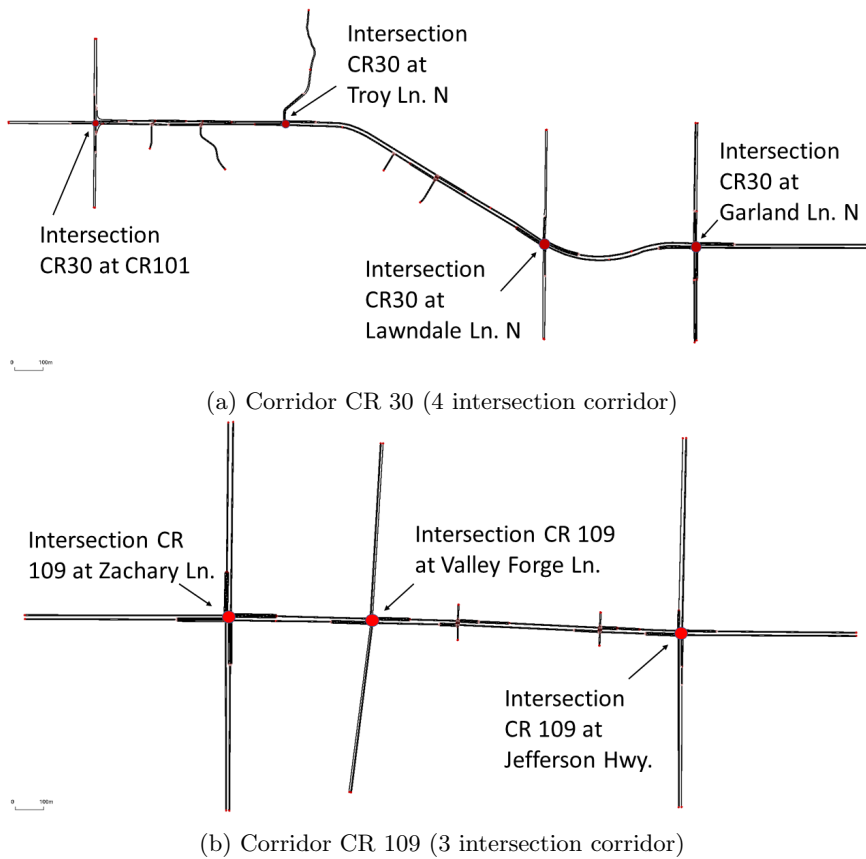


Figure 3.1: Intersections along CR 30 and CR 109 corridors.

signalized intersections along the County Road (CR) 30 and CR 109 corridors, respectively. These intersections were chosen by Hennepin County engineers to ensure the inclusion of variety of intersection geometries, level of services and different demand characteristics. The level of service achieved with the current AC signal control is shown in Table 3.1. The real-world demand data and traffic control logics from these intersections were used to create models and run simulations.

The simulation progression is tracked by time  $t$ . Yellow and red times from the current AC controllers include durations of 1-digit precision after the

Table 3.1: Level of service for County Road 30 corridor.

Intersection	AM peak	Mid-day peak	PM peak
CR 30 at CR 101	F	C	E
CR 30 at Troy Ln. N	A	A	A
CR 30 at Lawndale Ln. N	B	B	B
CR 30 at Garland Ln. N	B	B	C
CR 109 at Zachary Ln.	C/C	C/B	D/C
CR 109 at Valley Forge Ln.	A/A	A/A	A/A
CR 109 at Jefferson Hwy.	B/B	B/B	C/C

Table 3.2: Controller’s implemented in this thesis.

Controller	Abbreviation
Current actuated-coordinated signal controller	AC
Acyclic max-pressure controller (Varaiya, 2013)	AMP
Cyclic max-pressure controller without phase skipping (Levin et al., 2020)	CMP-NS
Cyclic max-pressure controller with phase skipping	CMP-S

decimal point which requires a simulation timestep of 0.1 second. The max-pressure time step can have an impact on the performance of max-pressure control. Therefore, we ran the simulations with 4 different max-pressure timesteps,  $\Delta t^{\text{MP}} \in \{5, 10, 15, 20\}$  seconds. For the AMP control, no cycle length was specified as that policy does not use cycle lengths. However, for the CMP controls a maximum cycle length  $\mathcal{C}_n^{\text{max}}$  for each node,  $n \in \mathcal{N}_i$  was specified before each simulation. To analyze the effects of different maximum cycle lengths on CMP controllers’ performance we used 4 different cycle lengths starting from the current AC control’s cycle length with increments of 30 seconds. Demand from 06:00 AM to 06:00 PM were divided into 10 and 9 simulation periods for the three and four intersection corridors respectively to carefully analyze performance of individual intersections on peak and off-peak periods separately.

Table 3.2 shows the list of signal controls implemented in this thesis. The simulations are created in the Simulation of Urban MObility (SUMO) by Lopez

et al. (2018) and the max pressure signal controls were implemented using the Python interface TraCI.

## 3.4 Simulation Results

First, we examine different max-pressure parameters to find the ones that improves the performance the most. We discuss the overall delay and throughput for each intersection during several demand periods in detail. Max-pressure controllers do not directly aim to reduce delay. Therefore, we focus on examining how max-pressure controls impact on delay. Then, we show how max-pressure control performs with the parameters that reduced delay the most. We compare the average delay and throughput for each control at all intersection at different periods. We also examine worst lane delays because this is where MP is expected to perform the worst as it may not activate a phase for a long time if pressure for the phase is not maximum. Finally, we discuss how the number of phase change is affected by different max-pressure controls. Monte Carlo simulations with 10 repetitions were used to increase robustness of the results.

### 3.4.1 Impact of Max-pressure Parameters

MP requires only one parameter which is the max-pressure timesteps. Along with max-pressure timesteps CMP requires another parameter which sets a maximum cycle length for an intersection. We ran simulations with 4 different max-pressure timesteps,  $\Delta t^{\text{MP}} \in \{5, 10, 15, 20\}$  seconds for all demand periods using the MP and CMP-S controllers. For CMP-S we also used 4 different maximum cycle lengths starting from the cycle length used in the AC signal controller with an increment of 30 seconds.

#### 3.4.1.1 Impact on Delay

The objective of max pressure control is to maximize throughput and it is not clear how delay is affected by different parameters of max-pressure control. We define delay as the time a vehicle spent on a lane with zero velocity. Figures 3.2 and 3.3 show a few heatmaps to demonstrate how different max-pressure parameters affected average delay. Delay for current AC signal control, AMP and CMP-S are also shown in those figures to show performance improvement from existing AC signal control. Only at intersection CR 30 at CR 101 during the PM peak CMP-S ended up increasing delays more than AC control. In all other cases CMP-S outperformed AC signal control using most of the combination of parameters.

No clear pattern was found for the change in delay due to the MP timestep and maximum cycle length parameters for CMP. In some cases, high MP timestep with low maximum cycle performed better like CR 30 at Garland Ln. N during PM peak. Higher MP timestep with lower maximum cycle reduces the number of times the optimal can be activated repeatedly to ensure all phases in the cycle get the chance to get activated. So, in these cases phase changes will be more frequent. That intersection also performs best with lower MP timestep using AMP which indicates that frequent phase changes increase performance there.

AMP only activates the optimal phases so vehicles waiting for other phases may experience high delays causing them to grow impatient and enter wrong lanes. While it is possible to keep the vehicles restricted at certain lanes using the simulator, vehicles in real life may grow impatient and enter wrong lanes. To make the simulations represent reality as closely as possible we do not force the vehicles to have infinite patience and drive perfectly. At shared lanes where a few vehicles in front of traffic queue want to make a different movement than the movement activated by optimal phase and very high demand for a few

movements can cause vehicles to enter wrong lanes. This causes error in the pressure calculations which leads to activating a sub-optimal phase. Using a CMP controller with higher MP-timestep can solve this problem to some extent. Because CMP-NS activates each phase in a cycle at least once and CMP-S also does the same when vehicles are waiting, using a CMP controller with higher MP-timestep may activate a phase for long enough to move the stuck vehicles. However, it will take more time to reach the next optimal phase if MP timestep is too high. Using high MP timestep will however cause problems if the maximum cycle length is not long enough to ensure activation of all phases in the cycle. Otherwise, an optimal phase may get interrupted or not even get the chance to be activated which would decrease performance.

The heatmaps show that after a certain increase in maximum cycle length more increase does not improve performance anymore. The max-pressure controllers seem to be more sensitive to MP timestep because different combination of maximum cycle length with the same timestep achieved the best performance several times in some intersections. In other cases only one combination of MP timestep and maximum cycle length achieved the highest performance.

Figure 3.4 shows how MP timestep affects average delays during different demand periods using AMP control. At the intersection of CR 30 at CR 101 delay during the PM peak period at 04:30 PM – 5:30 PM increase with increase in MP timestep. For the AM peak at that intersection during 07:00 AM – 08:00 AM delay decrease the most with increase in MP timestep up to 15 seconds. During all other periods delay decrease as MP timestep is increased up to 15 seconds and after that more increase in MP timestep results in increased delay. At CR 30 at Troy Ln. N during 04:30 PM – 05:30 PM which is the PM peak period for CR 30 at CR 101, delay increases with increase in MP timestep and during the 05:30 PM to – 06:00 PM period’s demand, delay fluctuates a lot with

change in MP timestep. Delay decreases as MP timestep is increased up to 15 seconds during the PM peak from 04:45 PM – 05:30 PM at this intersection. At CR 30 at Lawndale Ln. N during the AM periods delay slightly decreases with MP timestep increase and higher than 10 seconds of MP timestep end up increasing delay. At CR 30 at Garland Ln. N delays increase with timestep for all demand periods. During the AM peak at Zachary Ln. N delays first increased with increase in timestep up to 15 seconds and after that delays decreased. Increase in delay with higher MP timestep is also observed at CR 109 at Valley Forge Ln. N and Jefferson Hwy during most periods. AMP performed best using smaller MP timesteps except during the AM peak at CR 30 at CR 101.

#### **3.4.1.2 Impact on Throughput**

Figures 3.5 and 3.6 show the throughput at each intersection during different demand periods. CMP-S has to activate each phase in a cycle if vehicles are waiting for those phases. Because of this the the feasible region for CMP-S is smaller and it cannot directly activate the next optimal phase to maximize throughput. However, this activation of phases in sequence seems to be able to reduce delay more than it increases throughput. During the PM peak and off-peak and AM off-peak periods CMP could not increase throughput more than the current AC controls at the intersections of CR 30 at CR 101 and Troy Ln. N. AMP increased very small amount of throughput during the PM peak period at CR 30 at CR 101 and AM off-peak period at CR 30 at Troy Ln. N. During the AM peak however, both AMP and CMP-S were able to increase throughput more than current AC control. At Jefferson Hwy. both AMP and CMP-S failed to increase throughput except negligible increase at AM off-peak. CMP-S also could not outperform AC control during the AM peak at Zachary Ln. Both AMP and CMP-S were able to increase throughput in other conditions. At CR 30 at Lawndale Ln. N during PM peak and CR 30 at Garland Ln. N during the

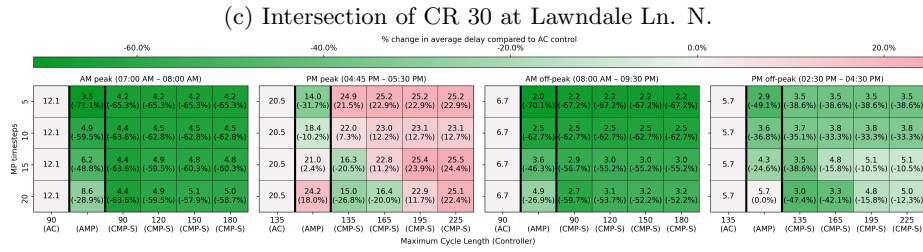
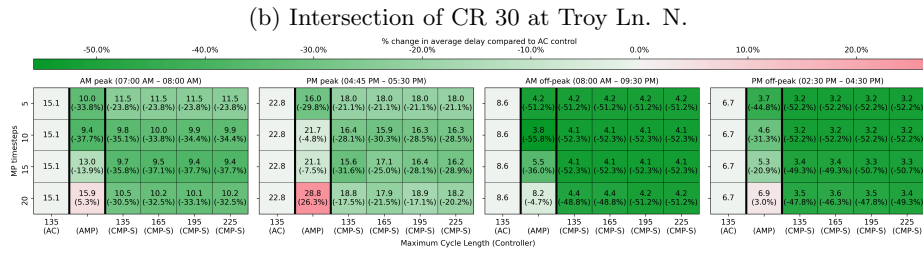
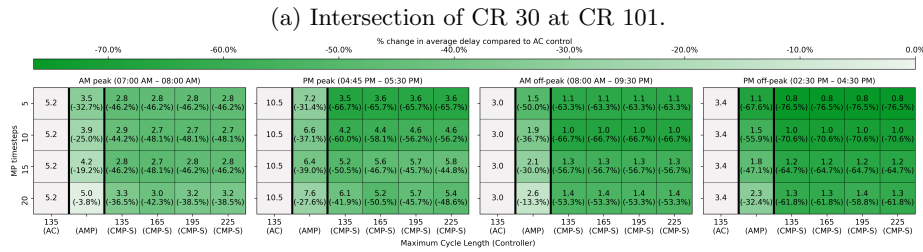
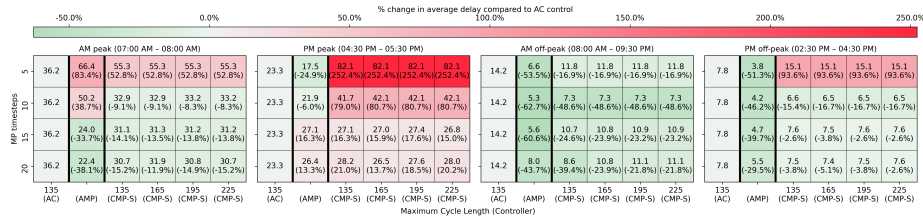


Figure 3.2: Average delay (in seconds) per vehicle per hour at the intersections along the CR 30 corridor during different demand periods.

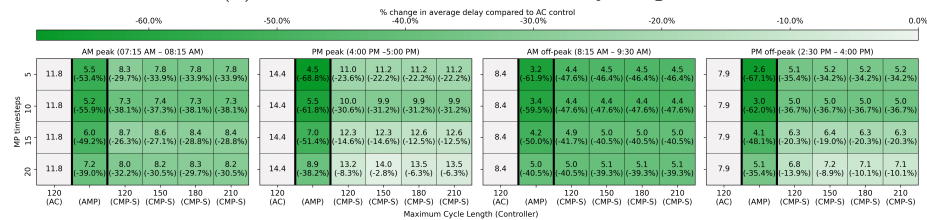
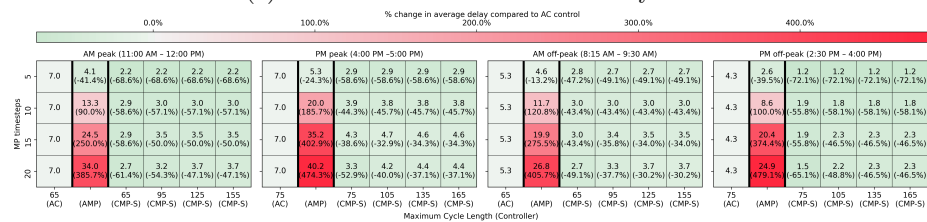
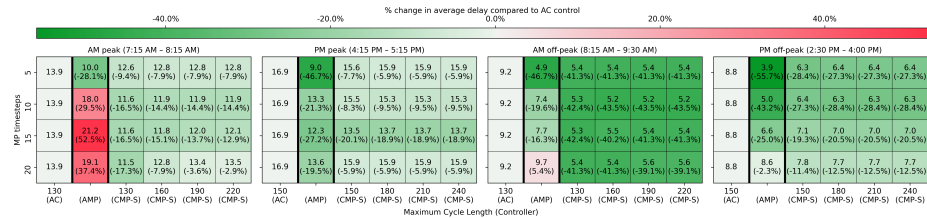


Figure 3.3: Average delay (in seconds) per vehicle per hour at the intersections along the CR 109 corridor during different demand periods.

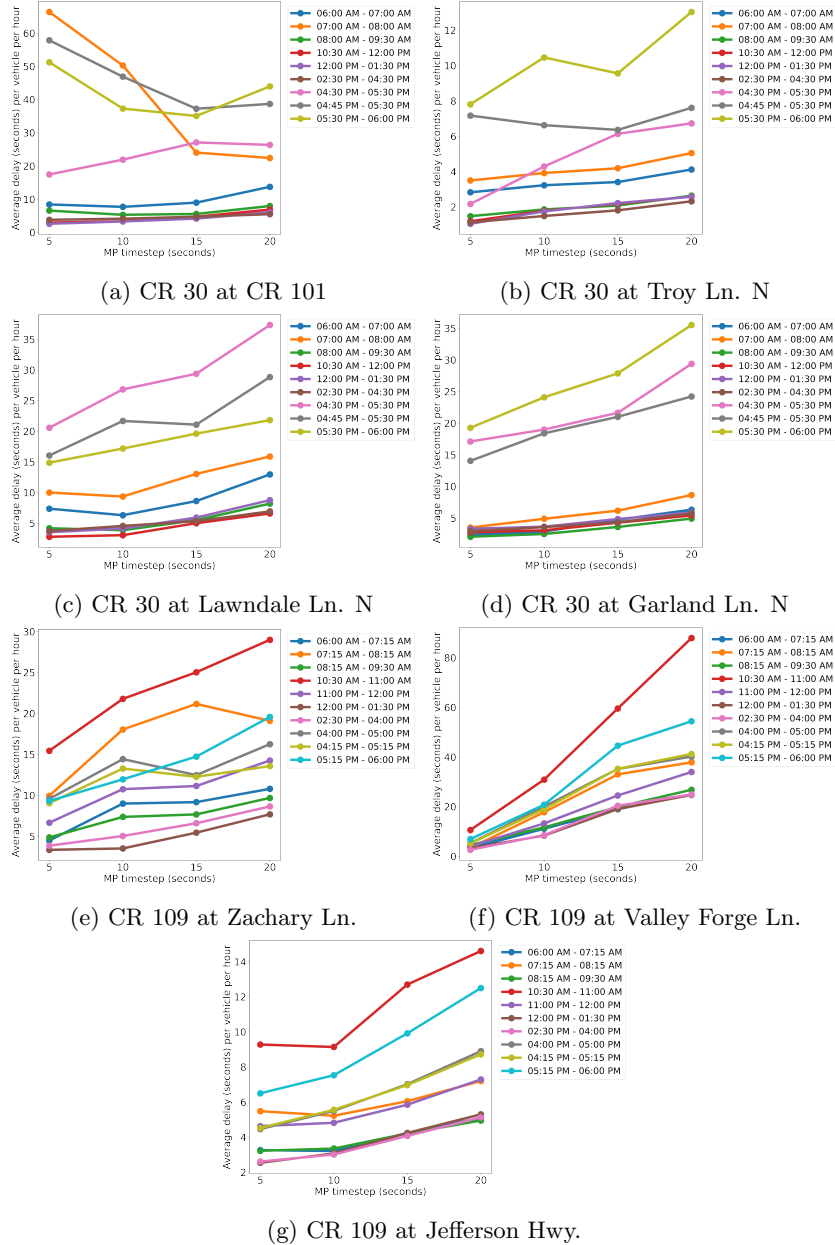


Figure 3.4: Effect of MP timesteps on average delay using AMP during different demand periods.

AM peak CMP-S ended up increasing more throughput than AMP. Even though throughput increase by using AMP and CMP-S is not very high compared to AC controls, significant delay reduction was observed for most cases.

### **3.4.2 Performance using Best Parameters**

We have selected the best MP timestep and maximum cycle length that reduced the most delay for each intersection for each demand period from the results from previous simulations using CMP-S controller. We use these parameters to run simulations again using CMP-S and CMP-NS. Because these parameters were selected based on the simulation results of CMP-S controller, results from CMP-NS using these parameters may not give the best delay reduction. For the AMP controller the MP timesteps that reduced the most delay were used for each intersection. Using the best parameters selected for individual intersections we examine the performance of the MP, CMP-NS and CMP-S. We also compare the results with current AC controls to determine if performance of the intersections can be increased.

#### **3.4.2.1 Delay**

Figure 3.7 shows the comparison between the average delays per vehicle per hour for each intersection under different demand periods along the 2 corridors.

AMP outperformed current AC control during all demand periods at all intersections by significant margins. Delays were higher for CMP-NS than for AMP for all cases. During several demand periods at intersections CR 30 at CR 101, Troy Ln. N, Garland Ln. N and at the intersections of CR 109 at Zachary Ln. and Valley Forge Ln. higher delays were observed in simulation compared to the current AC controller. At the intersection of CR 109 at Jefferson Hwy. during some periods delays slightly higher than AC controller's delay

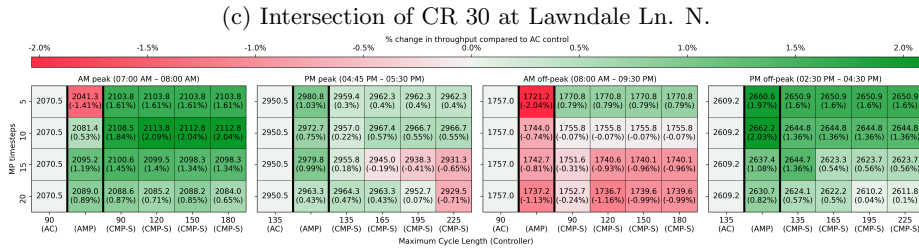
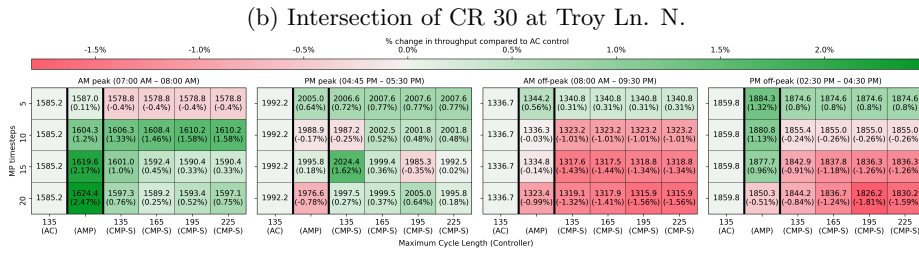
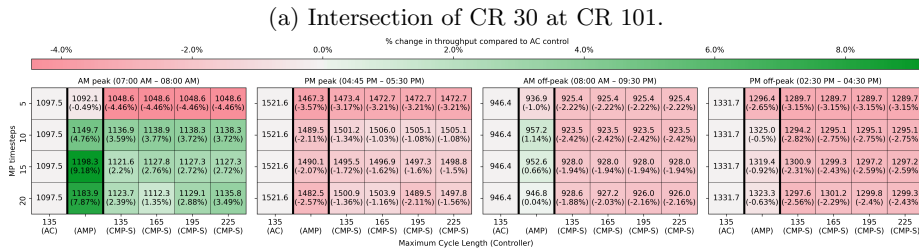
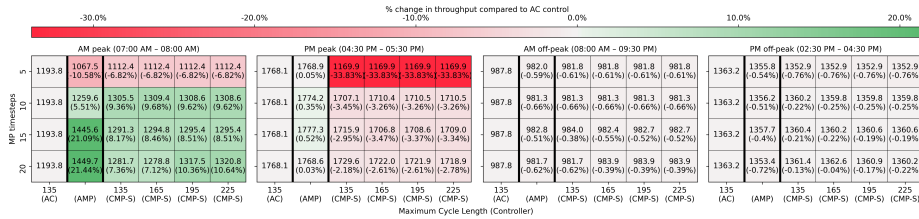
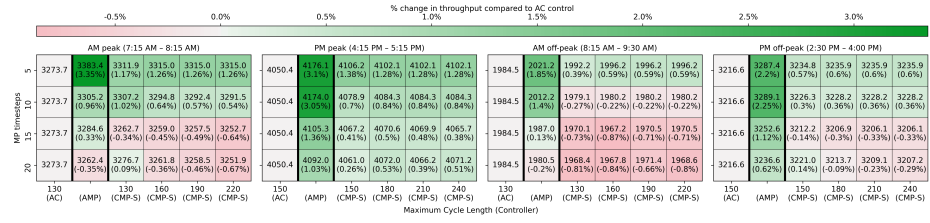
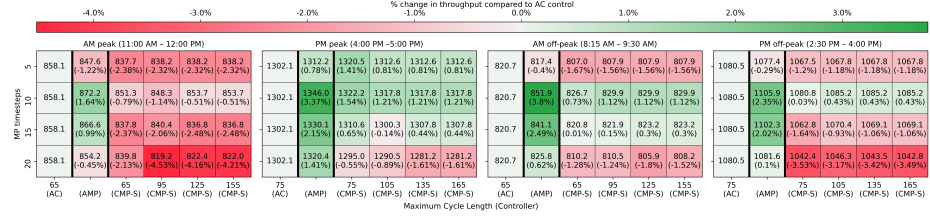


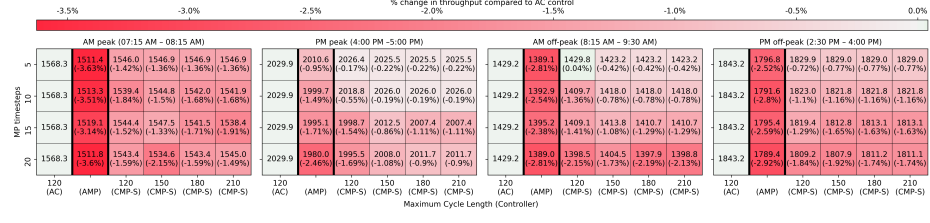
Figure 3.5: Throughput per hour at the intersections along the CR 30 corridor during different demand periods.



(a) Intersection of CR 109 at Zachary Ln.

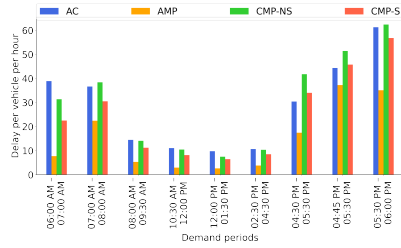


(b) Intersection of CR 109 at Valley Forge Ln.

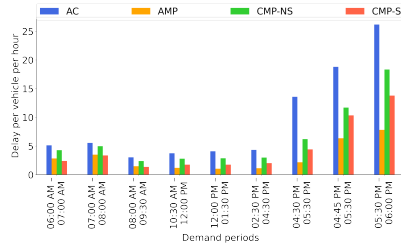


(c) Intersection of CR 109 at Jefferson Hwy.

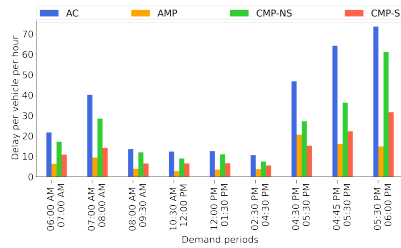
Figure 3.6: Throughput per hour at the intersections along the CR 109 corridor during different demand periods.



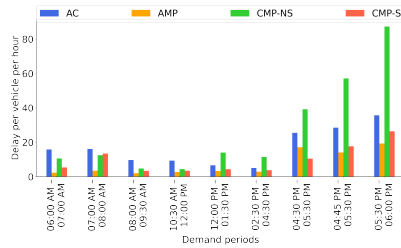
(a) CR 30 at CR 101



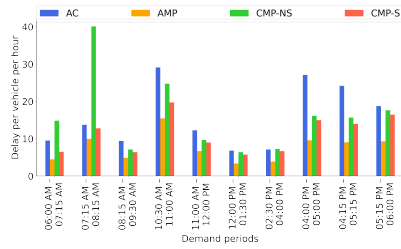
(b) CR 30 at Troy Ln. N



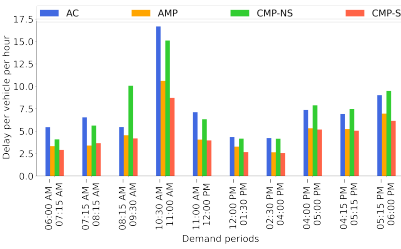
(c) CR 30 at Lawndale Ln. N



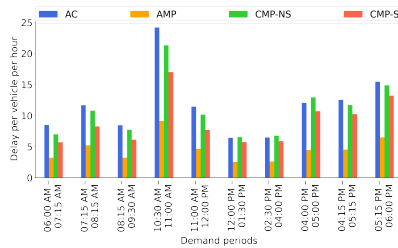
(d) CR 30 at Garland Ln. N



(e) CR 109 at Zachary Ln.



(f) CR 109 at Valley Forge Ln.



(g) CR 109 at Jefferson Hwy.

Figure 3.7: Average delays (in seconds) per vehicle per hour at intersections along CR 30 and CR 109.

were observed. Delays from CMP-S were higher than AMP controller's delays but CMP-S always outperformed AC controllers. Figure 3.7 also shows that CMP-S outperformed CMP-NS during most of the demand periods at different intersections.

Both CMP controllers performed worse than AMP in most situations because the feasible region of that control is constrained by the fact that, it must activate each phase at least once. CMP-S outperformed AC signal controllers in most cases while CMP-NS ended up increasing delays more than AC signal controllers for peak periods at several intersections. CMP-S increased delay under the PM peak demand periods at CR 30 at CR 101. Overall, the max-pressure controls decreased delays in most cases compared to current AC control. AMP reduced delay the most and CMP-S also outperformed the AC controllers most of the time.

#### 3.4.2.2 Throughput

The main objective of max-pressure control is maximizing the throughput by activating the phase with the highest pressure. Figure 3.8 compares the throughput achieved by different controllers. During the peak demand periods AMP and CMP-S performed better than AC controller in maximizing throughput for all intersections except CR 109 at Jefferson Hwy. At Jefferson Hwy. AMP performed the worst but throughput from the CMP controllers were very close to the AC controller's throughput. During the off-peak periods some AC controllers generated throughput more than the AMP and CMP-S controllers. However, the difference between the throughputs is very small as shown by the Figure 3.8. CMP-NS was able to create similar amount of throughput as the other controllers even with the restrictions that it had to activate each phase for at least the duration  $\Delta t^{\text{MP}}$ . In some cases, CMP-NS even generated the highest throughput of all the controllers. CMP-NS performed a little worse compared to

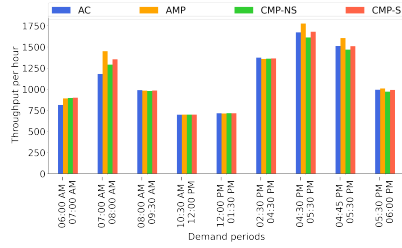
AMP and CMP-S during the peak periods. Overall, the throughputs using the max-pressure controllers were higher than the AC controllers during most of the demand periods and when AC controllers' throughput was higher the difference between throughputs from AC and max-pressure controllers were very small.

### **3.4.2.3 Worst Lane Delay**

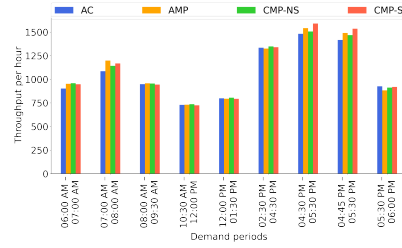
AMP only activates the optimal phases and skips any other phases in between. As a result vehicles waiting for those sub-optimal phases may end up waiting for a long time before their preferred phase is activated. This increases the delay for the vehicles waiting for those phases. That is why the worst lane's delay become very high for AMP. Figure 3.9 shows the percent change in worst lane's total delay per hour for the intersections along CR 30 and CR 109. For calculating the percent change the AC controller's worst lane's total delay is used as the baseline.

At the intersection of CR 109 at Jefferson Hwy. where AMP performed the worst in terms of throughput, worst lane delays seem to reduce compared to AC control. At CR 30 at CR 101 during the AM peak, PM peak and the last PM off-peak periods AMP increased worst lane's total delay. During the off-peak hours AMP was able to reduce worst lanes total delay more than AC control. At CR 30 at Troy Ln. N during the PM peaks AMP increased the worst lanes delay. At the intersections at CR 30 at Lawndale Ln. N, Garland Ln. N and the intersections along CR 109 at Zachary and Valley Forge Ln. AMP increased the worst lane delays.

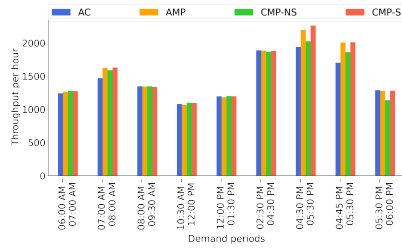
At intersections CR 30 at Garland Ln. N starting from the PM peak and at CR 30 at Zachary Ln. during the first AM off-peak, AM-peak and the from 02:30 PM – 06:00 PM, CMP-NS controller seem to increase the worst lane's delays. At intersections CR 30 at CR 101 during all periods it performed poorly and ended up increasing worst lane's delay. At the intersection of CR 109 and Zachary Ln.



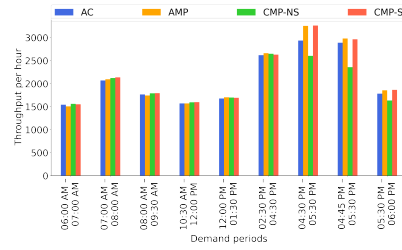
(a) CR 30 at CR 101



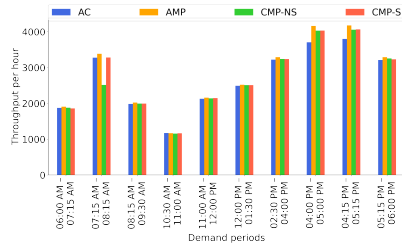
(b) CR 30 at Troy Ln. N



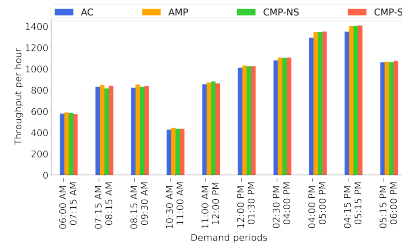
(c) CR 30 at Lawndale Ln. N



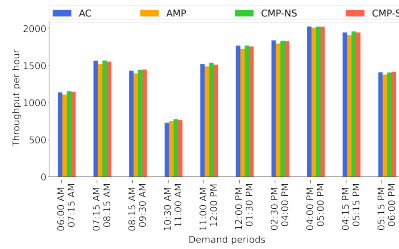
(d) CR 30 at Garland Ln. N



(e) CR 109 at Zachary Ln.



(f) CR 109 at Valley Forge Ln.



(g) CR 109 at Jefferson Hwy.

Figure 3.8: Throughput per hour at intersections along CR 30 and CR 109.

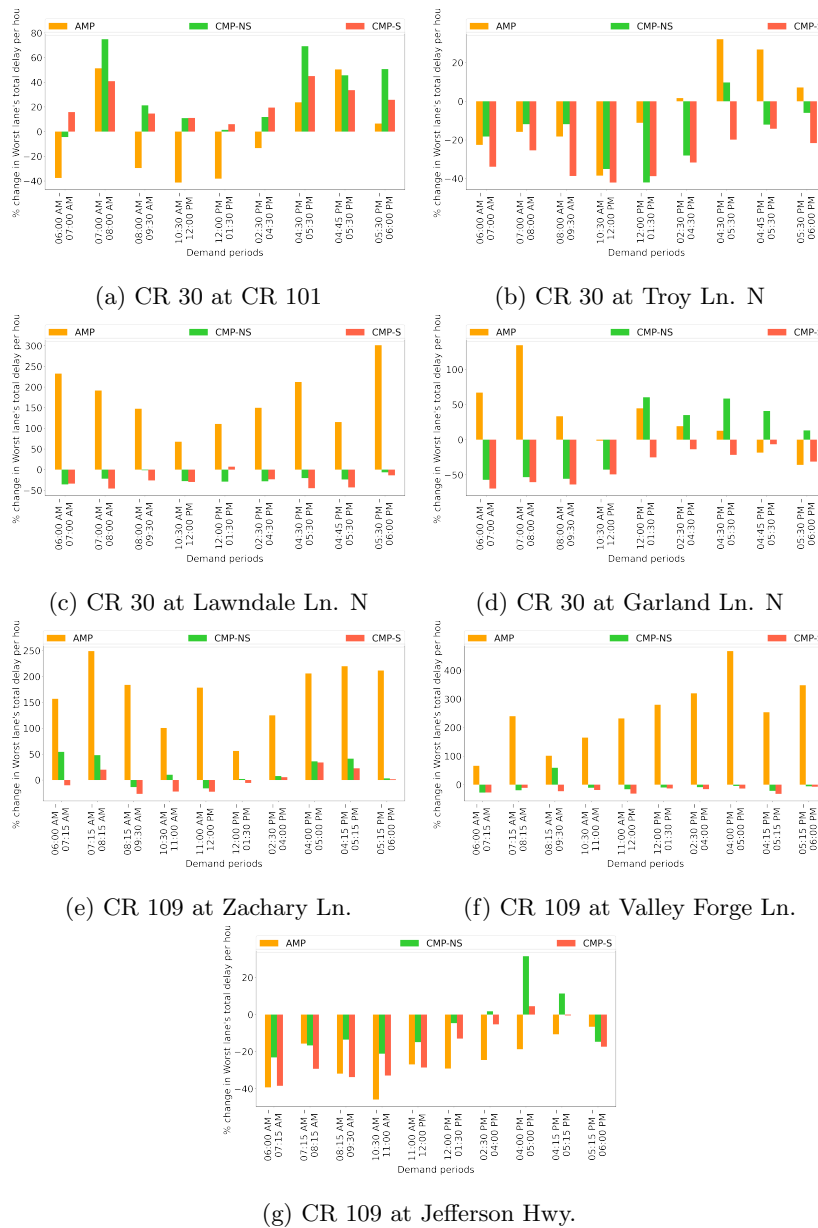


Figure 3.9: Percent change in worst lane's total delay per hour from AC signal controllers by max-pressure controllers along CR 30 and CR 109 corridors.

during 07:15 AM – 08:15 AM and 02:30 PM – 06:00 PM CMP-S increased worst lane’s delay instead of reducing it. CMP-S was able to reduce worst lane’s delay at most other intersections during different demand periods.

#### **3.4.2.4 Phase Changes**

The number of phase changes for different controllers are shown in Figure 3.10. For the max-pressure controllers the number of changes of phase varies with different demands. Because AMP activates only the optimal phases if traffic from some directions do not keep arriving at a higher rate increasing the pressure for those phases then AMP changes phases more frequently than AC signal controller.

Unlike AMP, the CMP controllers must activate phases in a consecutive order. So, if there are more phases between the current and the next optimal phase then CMP controllers must activate each of those intermediate phases before being able to activate the next optimal phase. This results in higher number of phase changes. CMP-NS does not activate the next phase if no vehicles are waiting for that phase so, number of phase changes should be lower for CMP-NS than CMP-S. However, the plots show that is not the case which means that there was at least one vehicle always waiting for the next phase. Phase changes is also affected by the max-pressure timesteps and maximum cycle lengths for the CMP controllers. Smaller maximum cycle lengths with high enough max-pressure timesteps will allow the optimal phase to be activated fewer times repeatedly which would cause phase changes.

CMP-S also move to the next phase as soon as all of the vehicles that want to use the current phase already left which increases the utilization of phases. Because of no more waiting vehicles if CMP-S tries to activate the next phase and the queue of phases is empty then max-pressure is called before the next MP timestep to determine the next optimal phase. CMP-S thus may call max-

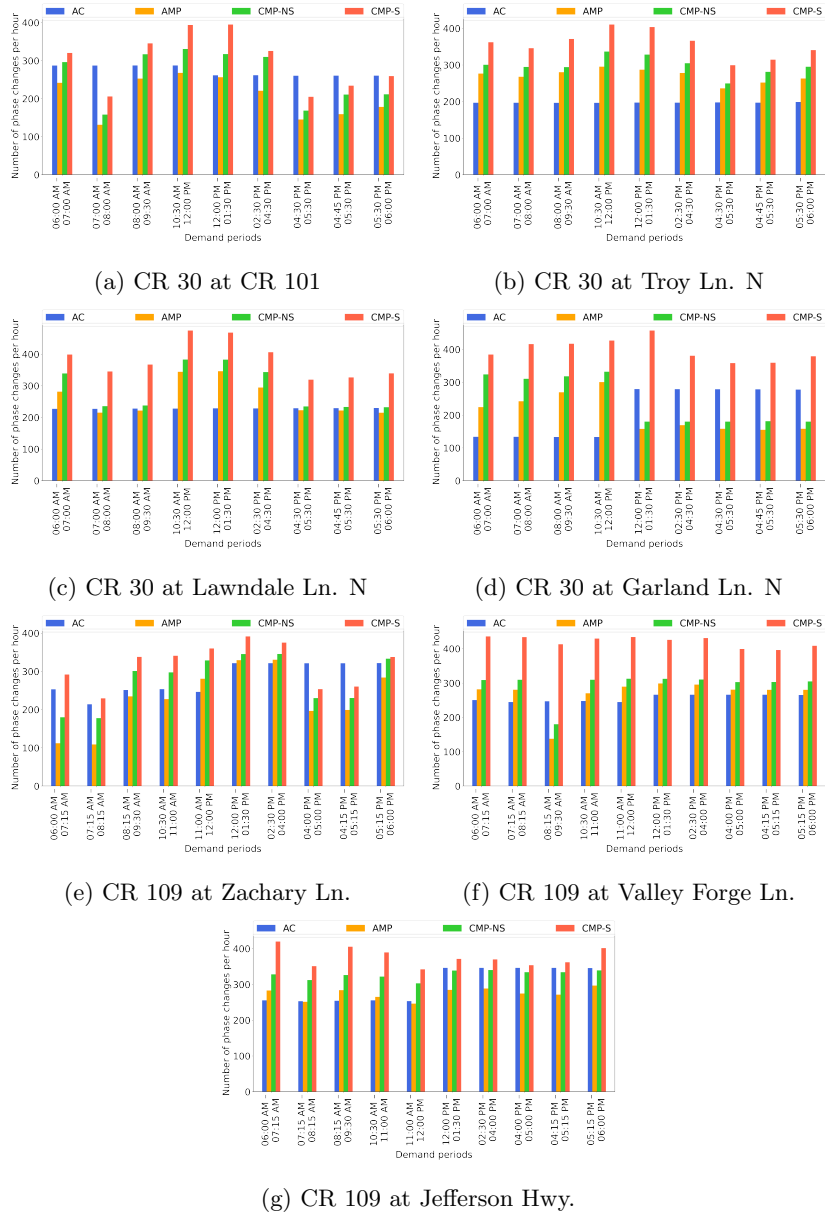


Figure 3.10: Number of phase changes per hour at the intersections along CR 30 and CR 109 under different demand periods.

pressure more times than CMP-NS for which the max-pressure is always scheduled to be called at the end of an MP timestep. For CMP-S this also means finding out the optimal phase and changing phases more often.

## Chapter 4

# Limited Deployment of MP Control

All the literature on MP control has analyzed the system performance with the assumption that MP control will be installed in all of the intersections of the network. However, in real life it may not be possible to install MP control in all intersections due to budgetary or other engineering limitations. The previous theoretical studies did not consider this in their proofs of stability. Currently there exists no numerical studies either on how network performance would be affected with only MP control installed in a limited number of intersections.

In this chapter, we introduce the limited deployment of MP controls policy formally. Then, we show that queue length can be bound or network can be stabilized under that policy. We also show that given a certain budget for upgrading intersection controls, limited deployment can maximally stabilize the traffic networks. We then formulate a mixed-integer-linear-program (MILP) to find the optimal intersections where MP control should be installed given a certain budget. We provide a greedy algorithm to solve the MILP and prove that

the algorithm can solve the problem to optimality efficiently. Then, we present numerical results that demonstrate a traffic network’s performance. We ran the simulations on the Downtown Austin network with calibrated signal timing and other data. To ensure high robustness we used multiple repetitions of Monte Carlo simulation. Finally, we conclude this chapter with the demonstration of advantages in terms of system performance with increasing budget for limited deployment of MP controls.

## 4.1 Notation and Terminology

We represent the traffic network as a directed graph where the intersections are the nodes of the graph. Two types of nodes are considered: 1. Nodes where MP control is installed and 2. Nodes where the existing pretimed traffic signal is installed. Then, we present the queuing model based on which the vehicle dynamics are determined. We use the point queue link model given by Vickrey (1963) with this queueing model. The point queue link model makes two assumptions about a link: 1. A link has a uncongestible physical section where vehicles can travel at freeflow speed and 2. A point queue at the downstream end of the link occupying no physical space where an infinite number of vehicles are allowed to stack up. The physical section represents the travel time on the link with no congestion and the point queue represents the delay due to congestion. Even though the point queue model does not completely capture traffic behaviour, a large amount of previous work (Varaiya, 2013; Le et al., 2015; Levin et al., 2019) used it to prove stability properties. This is mainly because with the point queue model it is easier to theoretically show that the network can still be stabilized. We define the limited deployment of MP control next. Then, the stable region or the set of demands that can be stabilized for any signal control with limited budget to modify traffic signals is defined.

We call that the stable region for limited deployment. Then, we show that for all demand in the stable region limited deployment of MP control is stable, meaning the sum of the queue lengths for the network will be bounded over a long period. We also show that if demand is not in the stable region network cannot be stabilized by any signal control.

Again, consider a directed graph,  $\mathcal{G} = (\mathcal{N}, \mathcal{A})$ . The sets of all nodes and links are denoted by  $\mathcal{N}$  and  $\mathcal{A} = \mathcal{A}_r \cup \mathcal{A}_i \cup \mathcal{A}_s$  respectively. Here,  $\mathcal{A}_r, \mathcal{A}_i$  and  $\mathcal{A}_s$  are the sets of entry, internal and exit links respectively.  $I(n)$  and  $O(n)$  are the sets of incoming and outgoing links from node  $n$  respectively.  $\mathcal{I}(i)$  and  $\mathcal{O}(i)$  are the sets of incoming and outgoing links to and from link  $i$  respectively. The tuple  $(i, j)$  represents a movement from link  $i$  to link  $j$ . Define the set of allowed movement via node  $n$  to be  $\mathcal{M}_n = \{(i, j) \mid \forall i \in I(n) \forall j \in O(n)\}$ .

Let  $\mathcal{N}^\pi \subseteq \mathcal{N}$  be the set of nodes where MP is installed and the rest of the nodes be  $\mathcal{N}^\sigma = \mathcal{N} \setminus \mathcal{N}^\pi$ , the set of nodes controlled by some other control policy. In other words, nodes in  $\mathcal{N}^\sigma$  have fixed traffic control that cannot be changed and nodes in  $\mathcal{N}^\pi$  will be controlled using MP control. While  $\mathcal{N}^\pi = \mathcal{N}$  meaning that all intersections are controlled with MP control is ideal, budget limitations may render it impractical. Furthermore, demand for some intersections may not be sufficiently large so that replacing the signal control with MP control would have any impactful practical benefit.

Before discussing traffic signal control policies we redefine the queuing model and describe how vehicles will move around throughout the network.

$$x_{ij}(t+1) = x_{ij}(t) - y_{ij}(t) + d_i(t)P_{ij}(t) \quad \forall i \in \mathcal{A}_r \quad \forall j \in \mathcal{O}(i) \quad (4.1)$$

$$x_{jk}(t+1) = x_{jk}(t) - y_{jk}(t) + \sum_{i \in \mathcal{I}(j)} y_{ij}(t)P_{jk}(t) \quad \forall j \in \mathcal{A}_i \cup \mathcal{A}_s \quad \forall k \in \mathcal{O}(j) \quad (4.2)$$

$$y_{ij}(t) = \min \{Q_{ij}S_{ij}(t), x_{ij}(t)\} \quad \forall n \in \mathcal{N} \quad \forall (i, j) \in \mathcal{M}_n \quad (4.3)$$

where  $d_i(t)$  and  $P_{ij}(t)$  are the exogenous demand coming into link  $i$  and turning proportions for movement  $(i, j)$  at time  $t$  respectively.  $Q_{ij}(t)$  represents the saturation rate and  $S_{ij}(t) \in \{0, 1\}$  represents whether the movement is inactive or active for the movement  $(i, j)$  at time  $t$ . Here equations (4.1) and (4.2) indicates that the queue length at the next time step is equal to the queue length minus the leaving vehicles plus the entering vehicles at the current time step. At most, the vehicles present at the queue  $x_{ij}(t)$  can leave the queue. Vehicles are allowed to leave the queue only if the signal is active or  $S_{ij}(t) = 1$ .  $y_{ij}(t)$  is the flow that is allowed to move at time step  $t$  and is determined by the minimum of the queue length and saturation rate if signal is active.

The queuing process is represented by  $\{\mathbf{x}(t) : t \geq 0\}$ . Here, the state at time  $t$  represented by  $\mathbf{x}(t) = \{x_{ij}(t) \forall n \in N \forall (i, j) \in \mathcal{M}_n\}$  depends on the signal control policy  $\phi : \mathbf{x}(t) \rightarrow S(t)$  and independent and identically distributed (iid) random vector  $\mathbf{d}(t)$  and matrix  $P(t)$ . The demand vector  $\mathbf{d}(t)$  at time  $t$  is a vector of random variables that represents the number of vehicles entering the network for all entry links at time  $t$ . The matrix  $P(t)$  describes the constant historical turn proportions for all movements in the network. Both  $\mathbf{d}(t)$  and  $P(t)$  are independent of the previous states  $x(t), \dots, x(1)$  of the system. Therefore, the next state only depends on the current state and some iid random variable  $h(\cdot)$  using the control  $\phi$ . Therefore, the queuing process can be written as

$$\mathbf{x}(t+1) = g_\phi(\mathbf{x}(t), h(\mathbf{d}(t), P(t))) \quad (4.4)$$

Again, since  $\mathbf{d}(t)$ ,  $P(t)$  are iid random variables and the function  $h(\cdot)$  maps to iid random variables, the queuing model is a Markov chain using the control  $\phi$ . This allows us to use different Markovian properties for our analysis in the next section.

## 4.2 Limited Deployment

Define the MP control, some other control and the limited deployment control policies with  $\pi, \sigma$  and  $\mu$  respectively. Let  $S_{ij}^\pi(t)$  and  $S_{ij}^\sigma(t)$  indicate whether signal is active for nodes in  $\mathcal{N}^\pi$  and nodes in  $\mathcal{N}^\sigma$  respectively for movement  $(i, j)$  at time  $t$ . At node  $n$ , time  $t$  signal activation for movement  $(i, j)$  with limited deployment policy  $\mu$  is defined as the following

$$S_{ij}^\mu(t) = \begin{cases} S_{ij}^\pi(t) & \text{if } n \in \mathcal{N}^\pi \\ S_{ij}^\sigma(t) & \text{if } n \in \mathcal{N}^\sigma \end{cases} \quad (4.5)$$

A network control matrix  $S(t) = [[S_{ij}(t) \forall j \in A] \forall i \in A]$  describes the signal activation status for all movements of the network at time  $t$ . With limited deployment of max pressure controllers, an intersection control matrix  $S_n(t) = [[S_{ij}(t) \forall j \in O(n)] \forall i \in I(n)]$  depends on the type of signal control that is installed at the intersection. Varaiya (2013) discusses these matrices in greater detail. Let  $\mathcal{S}$  and  $\mathcal{S}_n$  be the sets of all feasible network and intersection control matrices, and define the convex hull of  $\mathcal{S}$  as

$$\text{co}(\mathcal{S}) = \left\{ \sum_{S \in \mathcal{S}} \lambda_S S \mid \sum_{S \in \mathcal{S}} \lambda_S = 1, \lambda_S \geq 0 \right\} \quad (4.6)$$

where the fraction of activation time  $\lambda_S$  is given to each intersection control matrix  $S \in \mathcal{S}$ . We will use this definition of convex hull in the next section while analyzing the stable region and in the description of MP control.

The intersection control matrix using max pressure at time  $t$  can be obtained by solving the optimization problem (4.7) for all nodes in  $\mathcal{N}^\pi$ ,

$$S_n^\pi(t) = \arg \max_{S \in \text{co}(\mathcal{S}_n)} \left\{ \sum_{(i,j) \in \mathcal{M}_n} Q_{ij} S_{ij} w_{ij}(t) \right\} \quad (4.7)$$

with  $w_{ij}(t)$  defined by

$$w_{ij}(t) = x_{ij}(t) - \sum_{k \in \mathcal{O}(j)} x_{jk}(t) P_{jk} \quad (4.8)$$

here for each movement  $(i, j)$  a weight  $w_{ij}(t)$  is defined. MP control defines a pressure term for each combination of movements called a phase. The pressure term is the weighted sum of all the vehicles that are allowed to move during a phase. Here, MP control selects the network control matrix for which the total pressure for all movement is maximized. Varaiya (2013) showed that choosing a phase by maximizing this pressure term with the weight function defined in eq. (4.8) results in a signal control that can stabilize a network with stabilizable demand.

Assume that the sequence of intersection control matrices  $\{S_n^\sigma(t)\}_{t=1}^C$  with cycle length  $C$  is given. After every  $C$  timesteps the intersection control matrix at the beginning of that sequence is activated and then the rest of the sequence are followed in order. This other traffic signal controller can be the already existing traffic signal controller. For all nodes  $n \in \mathcal{N}^\sigma$  this other signal control should select the intersection control matrix  $S_n^\sigma(t)$  at time  $t$ .

**Lemma 1.** *The average network control matrix of some signal control policy  $\phi : x(t) \rightarrow S(t)$  is defined by*

$$\mathbb{S} = \lim_{T \rightarrow \infty} \frac{1}{T} \sum_{t=1}^T \phi(\mathbf{x}(t)) \quad (4.9)$$

and

$$\mathbb{S} \in \text{co}(\mathcal{S}) \quad (4.10)$$

*Proof.* Assume that over the time period  $T$ , the signal control matrices  $S_1, S_2,$

$\dots, S_m$  were activated for  $a_1, a_2, \dots, a_m$  times respectively. Now eq. (4.9) can be rewritten as

$$\mathbb{S} = \frac{\sum_{j=1}^m a_j S_j}{\sum_{i=1}^m a_i} = \frac{a_1 S_1}{\sum_{i=1}^m a_i} + \frac{a_2 S_2}{\sum_{i=1}^m a_i} + \dots + \frac{a_m S_m}{\sum_{i=1}^m a_i} \quad (4.11)$$

since  $a_j \geq 0$  is the number of times network control matrix  $S_j$  was activated and  $a_j \leq \sum_{i=1}^m a_i$  for all  $j \in \{1, \dots, m\}$ . Therefore, over total  $T$  time period the fraction of time  $\lambda_{S_j}$  signal control matrix  $S_j$  was activated is

$$\lambda_{S_j} = \frac{a_j}{\sum_{i=1}^m a_i} \geq 0 \quad \forall j \in \{1, \dots, m\} \quad (4.12)$$

and clearly,  $\sum_{S \in \mathcal{S}} \lambda_S = \sum_{j=1}^m \frac{a_j}{\sum_{i=1}^m a_i} = 1$ . So,  $\mathbb{S} \in \text{co}(\mathcal{S})$ .  $\square$

### 4.2.1 Stable region for limited deployment

We define the stable region to be the set of all demands that can be stabilized by some signal control. It is created by converting the average demand vector  $\bar{\mathbf{d}}$  using the turning proportions matrix  $\bar{P}$  to average link flow vector  $\bar{\mathbf{f}}$  and then checking whether a signal control can serve those demands on average. Define the feasible demands for the MP controller by

$$\mathcal{D}_\pi^\circ = \{ \mathbf{d} : (\bar{\mathbf{f}} = \bar{\mathbf{d}}\bar{P}) \wedge (\exists \mathbb{S} \in \text{co}(\mathcal{S}) \text{ s.t. } S_{ij} Q_{ij} > \bar{f}_i \bar{P}_{ij} \forall n \in \mathcal{N}^\pi, \forall (i, j) \in \mathcal{M}_n) \} \quad (4.13)$$

where the average network control matrix  $\mathbb{S} \in \text{co}(\mathcal{S})$ . This is proven in Lemma 1. Let the feasible demands for some other controller with average signal activation

$\bar{S}^\sigma$  represented by

$$\mathcal{D}_\sigma^\circ = \{ \mathbf{d} : (\bar{\mathbf{f}} = \bar{\mathbf{d}}\bar{P}) \wedge (\bar{S}_{ij}^\sigma Q_{ij} > \bar{f}_i \bar{P}_{ij} \quad \forall n \in \mathcal{N}^\sigma, \forall (i, j) \in \mathcal{M}_n) \} \quad (4.14)$$

Now we only allow modifying the control on nodes in  $\mathcal{N}^\pi$  and keep the controls on nodes in  $\mathcal{N}^\sigma$  unchanged. With this consideration the feasible demands for limited deployment can be defined as

$$\mathcal{D}_\mu^\circ = \left\{ \mathbf{d} : (\bar{\mathbf{f}} = \bar{\mathbf{d}}\bar{P}) \wedge \left( \exists \mathbb{S} \in \text{co}(\mathcal{S}) \text{ s.t. } \mathbb{S}_{ij} Q_{ij} > \bar{f}_i \bar{P}_{ij} \quad \forall n \in \mathcal{N}^\pi, \forall (i, j) \in \mathcal{M}_n \right. \right. \\ \left. \left. \wedge \bar{S}_{ij}^\sigma Q_{ij} > \bar{f}_i \bar{P}_{ij} \quad \forall n \in \mathcal{N}^\sigma, \forall (i, j) \in \mathcal{M}_n \right) \right\} \quad (4.15)$$

Therefore,  $\mathcal{D}_\mu^\circ \subseteq \mathcal{D}_\pi^\circ$ . We will show that if the average demand vector is in the stable region then limited deployment can stabilize the network. Otherwise, no signal controller can stabilize the network.

## 4.2.2 Stability with limited deployment

Before analyzing the stability of limited deployment we first define what stability means in Definition 1. If the average queue length for the entire network is bounded by some constant  $K < \infty$  then the network is said to be stable. Using the bound  $K$  we will further show that the average length of individual queues will also be bounded. Like Varaiya (2013) we will show that this bound does not depend on the network and only depends on the maximum values of demand and saturation rates.

**Definition 1.** *A network is stable if under average demand  $\bar{\mathbf{d}}$ , there exists a constant  $K < \infty$*

$$\lim_{T \rightarrow \infty} \mathbb{E} \left\{ \frac{1}{T} \sum_{t=1}^T \sum_{(i,j) \in \mathcal{A}^2} x_{ij}(t) \right\} < K \quad (4.16)$$

This definition of stability ensures that the total average queue length over a large period of time will be bounded. The total average queue length can only be bounded if each individual queue is also bounded on average. Each individual queue can be bounded if on average, service rate exceeds demand on each individual queue. We will show in Theorem 1 that if average demand vector  $\bar{\mathbf{d}}$  is in the stable region  $\mathcal{D}_\mu^\circ$  then with limited deployment control the network can be stabilized. Otherwise, if  $\bar{\mathbf{d}}$  is not in the stable region  $\mathcal{D}_\mu^\circ$  then there exists no control that can stabilize the network. That means limited deployment control can stabilize all possibly stabilizable demands and the only demands that it cannot stabilize, cannot be stabilized by any other control. That is referred to as the maximum stability property in the literature since it means that the control can stabilize the network for all possibly stabilizable demands.

**Theorem 1.** *Under the limited deployment of MP control policy  $\mu : \mathbf{x}(t) \rightarrow S(t)$ , the network is stable as per Definition 1 for average demand vector  $\bar{\mathbf{d}} \in \mathcal{D}_\mu^\circ$ .*

*Proof.* Define the Lyapunov function  $V : \mathbf{x}(t) \rightarrow \|\mathbf{x}(t)\|^2$  which maps the queue length vector to the sum of square of the queue lengths. The Lyapunov drift can be written as,

$$\Delta V(\mathbf{x}) = \mathbb{E} \{V(\mathbf{x}(t+1)) - V(\mathbf{x}(t)) \mid \mathbf{x}(t)\} = \mathbb{E} \{ \|\mathbf{x}(t+1)\|^2 - \|\mathbf{x}(t)\|^2 \mid \mathbf{x}(t) \} \quad (4.17)$$

Define  $\delta = \mathbf{x}(t+1) - \mathbf{x}(t)$ . Then,

$$\|\mathbf{x}(t+1)\|^2 - \|\mathbf{x}(t)\|^2 = 2\mathbf{x}(t)^T \delta + \|\delta\|^2 \quad (4.18)$$

Taking the expected value conditioned on  $\mathbf{x}(t)$

$$\Delta V(\mathbf{x}) = \mathbb{E} \{ \|\mathbf{x}(t+1)\|^2 - \|\mathbf{x}(t)\|^2 | \mathbf{x}(t) \} = 2\mathbb{E} \{ \mathbf{x}(t)^T \delta | \mathbf{x}(t) \} + \mathbb{E} \{ \|\delta\|^2 | \mathbf{x}(t) \} \quad (4.19)$$

According to Varaiya (2013),  $\mathbb{E} \{ \mathbf{x}^T \delta | \mathbf{x}(t) \}$  can be rewritten as

$$\begin{aligned} \mathbb{E} \{ \mathbf{x}^T \delta | \mathbf{x}(t) \} &= \sum_{i \in \mathcal{A}_t} \sum_{j \in \mathcal{O}(i)} w_{ij}(t) [ \bar{f}_i \bar{P}_{ij} - Q_{ij} S_{ij}(t) + Q_{ij} S_{ij}(t) \\ &\quad - \mathbb{E} \{ y_{ij}(t) | \mathbf{x}(t) \} ] \\ &= \alpha_1 + \alpha_2 \end{aligned} \quad (4.20)$$

Lemma 1 of Varaiya (2013) showed that  $\alpha_2$  is bounded if  $S_{ij}(t) \in \{0, 1\}$  for all  $(i, j) \in \mathcal{A}^2$ . Varaiya (2013) also showed that the bound for  $\alpha_2$  is a constant  $Mk_1$  where,  $M = |\cup_{n \in N} \mathcal{M}_n|$  is the total number of queues. The bound for  $\alpha_1$  is  $\alpha_1 \leq -\epsilon\eta \|\mathbf{x}(t)\|$  which is derived in Lemma 3 where  $\eta > 0$ .

$$\alpha_1 + \alpha_2 \leq -\epsilon\eta \|\mathbf{x}(t)\| + Mk_1 \quad (4.21)$$

Varaiya (2013) showed that  $\mathbb{E} \{ \beta | \mathbf{x}(t) \} = \mathbb{E} \{ \|\delta\|^2 | \mathbf{x}(t) \}$  is bounded by  $Mk_2^2$  where,  $k_2$  depends on the saturation rates and the maximum values of the demands.

$$\Delta V(\mathbf{x}) = \mathbb{E} \{ \|\mathbf{x}(t+1)\|^2 - \|\mathbf{x}(t)\|^2 | \mathbf{x}(t) \} \leq -\epsilon\eta \|\mathbf{x}(t)\| + Mk_1 + Mk_2^2 \quad (4.22)$$

Taking the unconditional expectation we get

$$\mathbb{E} \{ \|\mathbf{x}(t+1)\|^2 \} - \mathbb{E} \{ \|\mathbf{x}(t)\|^2 \} \leq K - \epsilon\eta \mathbb{E} \{ \|\mathbf{x}(t)\| \} \leq K - \epsilon \mathbb{E} \{ \|\mathbf{x}(t)\| \} \quad (4.23)$$

Summing over  $t \in T$

$$\begin{aligned}
\sum_{t \in T} K - \epsilon \sum_{t \in T} \mathbb{E} \|\mathbf{x}(t)\| &\geq \sum_{t \in T} (\mathbb{E} \|\mathbf{x}(t+1)\|^2 - \mathbb{E} \|\mathbf{x}(t)\|^2) \\
\implies KT - \epsilon \sum_{t \in T} \mathbb{E} \|\mathbf{x}(t)\| &\geq \mathbb{E} \|\mathbf{x}(2)\|^2 + \mathbb{E} \|\mathbf{x}(3)\|^2 + \dots + \mathbb{E} \|\mathbf{x}(T+1)\|^2 \\
&\quad - (\mathbb{E} \|\mathbf{x}(1)\|^2 + \mathbb{E} \|\mathbf{x}(2)\|^2 + \dots + \mathbb{E} \|\mathbf{x}(T)\|^2) \\
\implies \epsilon \frac{1}{T} \sum_{t \in T} \mathbb{E} \|\mathbf{x}(t)\| &\leq K + \frac{1}{T} \mathbb{E} \|\mathbf{x}(1)\|^2 - \frac{1}{T} \mathbb{E} \|\mathbf{x}(T+1)\|^2 \\
&\leq K + \frac{1}{T} \mathbb{E} \|\mathbf{x}(1)\|^2
\end{aligned}$$

which implies stability as per Definition 1.  $\square$

Theorem 1 proves that under limited deployment of MP controllers, average queue length over long run will be bounded if  $\bar{\mathbf{d}} \in \mathcal{D}_\mu^\circ$ . That means, more vehicles can be served with limited deployment than average demand. So any demand  $\bar{\mathbf{d}} \in \mathcal{D}_\mu^\circ$  can be served without causing the queues to grow to infinity with limited deployment. Therefore, limited deployment satisfies eq. (4.16) which makes it a stable control policy for any demand  $\bar{\mathbf{d}} \in \mathcal{D}_\mu^\circ$ . Following the arguments of remark 2 of Varaiya (2013), from (4.22) it can further be shown that average queue length of any individual queue in equilibrium is bounded by

$$\frac{1}{M} \mathbb{E} \{\mathbf{x}(t)\} \leq \frac{k_1 + k_2^2}{\epsilon} \tag{4.24}$$

Where,  $k_1$  and  $k_2$  are constants that depend only on the saturation rates and the maximum demand, and not the network.

To prove Lemma 2 we will use an established result given in Theorem 2 Hoffman and Kruskal (2016). Properties of totally unimodular matrices are used in Theorem 2. So, we give the definition of totally unimodular matrices in Definition 2 before stating the Theorem 2.

**Definition 2.** Matrix  $A \in \mathbb{R}^{m \times n}$  is totally unimodular (TU) if  $\det(\text{SS}_i(A)) \in \{-1, 0, +1\}$  for all  $i$  where,  $\text{SS}_i$  is the  $i$ th square submatrix of  $A$ .

**Theorem 2** (Hoffman-Kruskal theorem Hoffman and Kruskal (2016)). If  $A$  is TU and  $b$  is an integer vector then, polytope  $P = \{x : Ax \leq b\}$  has only integer vertices.

**Lemma 2.**

$$\max_{S \in \mathcal{S}} \left\{ \sum_{(i,j) \in \mathcal{M}_n} S_{ij} Q_{ij} w_{ij}(t) \right\} = \max_{\mathbb{S} \in \text{co}(\mathcal{S})} \left\{ \sum_{(i,j) \in \mathcal{M}_n} \mathbb{S}_{ij} Q_{ij} w_{ij}(t) \right\} \quad \forall n \in \mathcal{N}^\pi \quad (4.25)$$

*Proof.* The convex hull can be written as

$$\text{co}(\mathcal{S}) = \left\{ \sum_{S \in \mathcal{S}} \lambda_S S \mid A^T \lambda = \mathbf{b}, \lambda_S \geq 0 \forall S \in \mathcal{S} \right\} \quad (4.26)$$

where

$$A = \begin{bmatrix} 1 \\ 1 \\ \vdots \\ 1 \end{bmatrix} \in \mathbb{R}^{|\mathcal{S}| \times 1} \quad \lambda = \begin{bmatrix} \lambda_1 \\ \lambda_2 \\ \vdots \\ \lambda_{|\mathcal{S}|} \end{bmatrix} \in \mathbb{R}^{|\mathcal{S}| \times 1} \quad b = 1 \quad (4.27)$$

Here,  $\det(\text{SS}_i(A)) = 1 \in \{-1, 0, +1\}$ . According to theorem 2  $A$  is TU and  $b = 1$  is integer. So, the polytope  $\text{co}(\mathcal{S})$  only has integer vertices or extreme points.

According to the Linear Programming (LP) Fundamental Theorem (Chong and Zak, 2004), if there is an optimal solution then there is an optimal solution that is a basic feasible solution (BFS). For a standard LP polytope

$\{\lambda : A^T \lambda = \mathbf{b}, \lambda \geq 0\}$ ,  $\lambda$  is a BFS if and only if  $\lambda$  is an extreme point. Since, all BFS's in the polytope  $\text{co}(\mathcal{S})$  are integers there exists an optimal solution with entries  $S_{ij}$  in  $\{0, 1\}$  for all  $(i, j) \in \mathcal{M}_n$  for all  $n \in \mathcal{N}$ .

□

**Lemma 3.**

$$\alpha_1 \leq -\epsilon\eta \|\mathbf{x}(t)\| \quad (4.28)$$

*Proof.* Define the max pressure policy by  $\pi : \mathbf{x}_n(t) \rightarrow S_n^\pi(t)$ , some other signal control policy  $\sigma : \mathbf{x}_n(t) \rightarrow S_n^\sigma(t)$ . Now the limited deployment policy can be defined by  $\mu : \mathbf{x}_n(t) \rightarrow S_n^\mu(t)$ . Since  $\pi$  maximizes pressure, any other controller  $\sigma$  can not result in more pressure from the signal.

$$\sum_{n \in \mathcal{N}} \sum_{(i,j) \in \mathcal{M}_n} S_{ij}^\pi(t) Q_{ij} w_{ij}(t) \geq \sum_{n \in \mathcal{N}} \sum_{(i,j) \in \mathcal{M}_n} S_{ij}^\sigma(t) Q_{ij} w_{ij}(t) \quad (4.29)$$

With limited deployment, MP only controls nodes where MP is installed and on other nodes we assume the signal timing is exogenous represented by  $S^\sigma$ .

$$\begin{aligned} \sum_{n \in \mathcal{N}} \sum_{(i,j) \in \mathcal{M}_n} S_{ij}^\mu(t) Q_{ij} w_{ij}(t) &= \sum_{n \in \mathcal{N}^\pi} \sum_{(i,j) \in \mathcal{M}_n} S_{ij}^\pi(t) Q_{ij} w_{ij}(t) \\ &+ \sum_{n \in \mathcal{N}^\sigma} \sum_{(i,j) \in \mathcal{M}_n} S_{ij}^\sigma(t) Q_{ij} w_{ij}(t) \end{aligned} \quad (4.30)$$

Therefore,

$$\begin{aligned} \sum_{n \in \mathcal{N}} \sum_{(i,j) \in \mathcal{M}_n} S_{ij}^\pi(t) Q_{ij} w_{ij}(t) &\geq \sum_{n \in \mathcal{N}} \sum_{(i,j) \in \mathcal{M}_n} S_{ij}^\mu(t) Q_{ij} w_{ij}(t) \\ &\geq \sum_{n \in \mathcal{N}} \sum_{(i,j) \in \mathcal{M}_n} S_{ij}^\sigma(t) Q_{ij} w_{ij}(t) \end{aligned} \quad (4.31)$$

Now by Lemma 2 and the definition of MP control, when  $N^\pi = N$

$$\begin{aligned} \sum_{(i,j) \in \mathcal{M}_n} S_{ij}^\pi(t) Q_{ij} w_{ij}(t) &= \max_{S \in \mathcal{S}} \left\{ \sum_{(i,j) \in \mathcal{M}_n} Q_{ij} S_{ij} w_{ij}(t) \right\} \\ &= \max_{S \in \text{co}(\mathcal{S})} \left\{ \sum_{(i,j) \in \mathcal{M}_n} Q_{ij} S_{ij} w_{ij}(t) \right\} \end{aligned} \quad (4.32)$$

By eqs. (4.30) and (4.32)

$$\begin{aligned} \sum_{n \in \mathcal{N}} \sum_{(i,j) \in \mathcal{M}_n} S_{ij}^\mu(t) Q_{ij} w_{ij}(t) &= \max_{S \in \text{co}(\mathcal{S})} \left\{ \sum_{(i,j) \in \mathcal{M}_n} Q_{ij} S_{ij} w_{ij}(t) \right\} \\ &\quad + \sum_{n \in \mathcal{N}^\sigma} \sum_{(i,j) \in \mathcal{M}_n} S_{ij}^\sigma(t) Q_{ij} w_{ij}(t) \end{aligned} \quad (4.33)$$

When  $d \in D_\mu^\circ$  then for all  $n \in \mathcal{N}^\pi$  there exists  $S \in \text{co}(\mathcal{S})$  such that

$$S_{ij} Q_{ij} = \begin{cases} \bar{f}_i \bar{P}_{ij} + \epsilon & \text{if } w_{ij}(t) > 0 \\ 0 & \text{if } w_{ij}(t) \leq 0 \end{cases}$$

$$\bar{S}_{ij}^\sigma Q_{ij} = \begin{cases} \bar{f}_i \bar{P}_{ij} + \epsilon & \text{if } w_{ij}(t) > 0 \\ 0 & \text{if } w_{ij}(t) \leq 0 \end{cases}$$

here  $\bar{S}^\sigma$  is the average exogenous signal control.

$$\begin{aligned}
\alpha_1 &= \sum_{n \in \mathcal{N}} \sum_{(i,j) \in \mathcal{M}_n} [\bar{f}_i \bar{P}_{ij} - \bar{S}_{ij}^\mu Q_{ij}] w_{ij}(t) \\
&= \sum_{n \in \mathcal{N}^\pi} \sum_{(i,j) \in \mathcal{M}_n} [\bar{f}_i \bar{P}_{ij} - \mathbb{S}_{ij} Q_{ij}] w_{ij}(t) \\
&\quad + \sum_{n \in \mathcal{N}^\sigma} \sum_{(i,j) \in \mathcal{M}_n} [\bar{f}_i \bar{P}_{ij} - \bar{S}_{ij}^\sigma Q_{ij}] w_{ij}(t) \\
&= \sum_{n \in \mathcal{N}^\pi} \sum_{(i,j) \in \mathcal{M}_n} [-\epsilon w_{ij}(t)^+ + \bar{f}_i \bar{P}_{ij} w_{ij}(t)^-] \\
&\quad + \sum_{n \in \mathcal{N}^\sigma} \sum_{(i,j) \in \mathcal{M}_n} [-\epsilon w_{ij}(t)^+ + \bar{f}_i \bar{P}_{ij} w_{ij}(t)^-] \\
&= \sum_{n \in \mathcal{N}} \sum_{(i,j) \in \mathcal{M}_n} [-\epsilon w_{ij}(t)^+ + \bar{f}_i \bar{P}_{ij} w_{ij}(t)^-] \leq -\epsilon \sum_{n \in \mathcal{N}} \sum_{(i,j) \in \mathcal{M}_n} |w_{ij}(t)|
\end{aligned}$$

According to Varaiya (2013) since the map  $w : \mathbf{x} \rightarrow \mathbb{R}$  is injective there exists  $\eta > 0$  such that

$$\sum_{n \in \mathcal{N}} \sum_{(i,j) \in \mathcal{M}_n} |w_{ij}(t)| \geq \eta \|\mathbf{x}(t)\| \tag{4.34}$$

Therefore,  $\alpha_1 \leq -\epsilon \eta \|\mathbf{x}(t)\|$  □

**Theorem 3.** *There does not exist any signal control under limited budget that can stabilize a network with average demand vector  $\bar{\mathbf{d}} \notin \mathcal{D}_\mu^\circ$*

*Proof.* If  $\bar{\mathbf{d}} \notin \mathcal{D}_\mu^\circ$  then we get  $\bar{\mathbf{d}} \in \tilde{\mathcal{D}}_\mu$ . When  $\bar{\mathbf{d}}$  is on the boundary of  $\mathcal{D}_\mu^\circ$  the Markov chain representing the queuing model can be null recurrent. For stability the Markov chain is required to be positive recurrent which is implied

by Definition 1. So, we consider only the interior  $\mathcal{D}'_\mu$  of  $\tilde{\mathcal{D}}_\mu$ . Then, we get

$$\mathcal{D}'_\mu = \left\{ \mathbf{d} : (\bar{\mathbf{f}} = \mathbf{d}\bar{P}) \wedge \left( \forall \mathbb{S} \in \text{co}(\mathcal{S}), \forall n \in \mathcal{N}^\pi, \exists (i, j) \in \mathcal{M}_n \text{ s.t. } \mathbb{S}_{ij} Q_{ij} < \bar{f}_i \bar{P}_{ij}, \right. \right. \\ \left. \left. \wedge \forall n \in \mathcal{N}^\sigma, \exists (i, j) \in \mathcal{M}_n \text{ s.t. } \bar{S}_{ij}^\sigma Q_{ij} < \bar{f}_i \bar{P}_{ij} \right) \right\} \quad (4.35)$$

For link  $i \in A \setminus \mathcal{A}_r$  the flow is  $f_i(t) = \sum_{h \in \mathcal{I}(i)} y_{hi}(t)$  and Varaiya (2013) showed that the flow for link  $i \in \mathcal{A}_r$  is  $f_i(t) = d_i(t)$ . Therefore, we can generalize the queueing process given in eqs. (4.1) and (4.2) as the following

$$x_{ij}(t+1) = x_{ij}(t) + f_i(t)P_{ij}(t) - y_{ij}(t) \quad \forall i \in A \forall j \in O(i) \quad (4.36)$$

Taking the expected value we get

$$\mathbb{E} \{x_{ij}(t+1) - x_{ij}(t)\} = \mathbb{E} \{f_i(t)P_{ij}(t) - y_{ij}(t)\} \quad (4.37)$$

$$\implies \mathbb{E} \{x_{ij}(t+1) - x_{ij}(t)\} = \mathbb{E} \{f_i(t)P_{ij}(t) - \min \{x_{ij}(t), S_{ij}^\mu(t)Q_{ij}\}\} \quad (4.38)$$

Now for any demand vector  $\bar{\mathbf{d}} \in \mathcal{D}'_\mu$  there exists a movement  $(i, j)$  such that

$$\mathbb{E} \{x_{ij}(t+1) - x_{ij}(t)\} > \bar{f}_i \bar{P}_{ij} - \bar{S}_{ij}^\mu Q_{ij} > 0 \quad (4.39)$$

However, equation (4.39) implies increasing queue length at every timestep on average for at least one movement  $(i, j)$  which violates Definition 1. Therefore if  $\bar{\mathbf{d}} \notin \mathcal{D}_\mu^\circ$  the network cannot be stabilized by any control.  $\square$

**Corollary 1.** *Limited deployment control is maximally stable.*

*Proof.* Theorem 1 showed that if  $\bar{\mathbf{d}} \in \mathcal{D}_\mu^\circ$  then the limited deployment can stabilize the network. Theorem 3 showed that if  $\bar{\mathbf{d}} \notin \mathcal{D}_\mu^\circ$  then no control can

stabilize the network. Therefore, limited deployment control can stabilize all possibly stabilizable demands.  $\square$

### 4.3 Limited Deployment Formulation

Having shown that under limited deployment  $\mathcal{N} = \mathcal{N}^\sigma \cup \mathcal{N}^\pi$ , max-pressure control will stabilize any demand  $\bar{\mathbf{d}}$  in the restricted stability region  $\mathcal{D}_\mu^\circ$  the natural objective is to select  $\mathcal{N}^\pi \subseteq \mathcal{N}$  to optimize  $\mathcal{D}_\mu^\circ$ . While  $\mathcal{N}^\pi = \mathcal{N}$  is ideal, budget limitations may render it impractical. Furthermore, demand for some intersections may be sufficiently small that replacing their signal control hardware has little practical benefit. We formulate a mixed integer linear program to identify the highest-priority intersections to implement max-pressure control.

#### 4.3.1 Demand Maximization Under Limited Budget

Let  $\gamma_n \in \{0, 1\}$  indicate whether the intersection control at node  $n$  is updated, and let  $b_n$  be the cost of updating node  $n$  with a total budget limitation of  $B$ . If  $n$  is updated, then the default control at  $n$  of  $\tilde{S}_n$  can be replaced with some  $\bar{S}_n \in \text{co}(\mathcal{S}_n)$ . This choice can be represented by the following constraints.

$$\bar{f}_i = \bar{d}_i \quad \forall i \in \mathcal{A}_r \quad (4.40a)$$

$$\bar{f}_j = \sum_{i \in I(n)} \bar{f}_i \bar{P}_{ij} \quad \forall j \in \mathcal{A}_i \cup \mathcal{A}_s \quad (4.40b)$$

$$f_i P_{ij} \leq Q_{ij} \bar{S}_{ij} \quad \forall n \in \mathcal{N}, \forall i \in I(n), \forall j \in \mathcal{O}(i) \quad (4.40c)$$

$$\bar{S}_{ij} = \sum_{S \in \mathcal{S}_n} \lambda_S S_{ij} \quad \forall n \in \mathcal{N}, \forall i \in I(n), \forall j \in \mathcal{O}(i) \quad (4.40d)$$

$$\sum_{S \in \mathcal{S}_n} \lambda_S \leq 1 \quad \forall n \in \mathcal{N} \quad (4.40e)$$

$$\gamma_n \geq \bar{S}_{ij} - \tilde{S}_{ij} \quad \forall n \in \mathcal{N}, \forall i \in I(n), \forall j \in \mathcal{O}(i) \quad (4.40f)$$

$$\gamma_n \geq \tilde{S}_{ij} - \bar{S}_{ij} \quad \forall n \in \mathcal{N}, \forall i \in I(n), \forall j \in \mathcal{O}(i) \quad (4.40g)$$

$$\gamma_n \in \{0, 1\} \quad \forall n \in \mathcal{N} \quad (4.40h)$$

Constraint (4.40c) is the stable region constraint used in eq. (4.15), and constraints (4.40d) and (4.40e) relate  $\bar{S}_{ij}$  to the definition of the convex hull. Constraints (4.40f) and (4.40g) force  $\gamma_n = 1$  if  $\bar{S}_{ij} \neq \tilde{S}_{ij}$  (i.e. the signal timing is changed due to implementing max-pressure control). The budget constraint can be written as

$$\sum_{n \in \mathcal{N}} b_n \gamma_n \leq B \quad (4.41)$$

If the objective is to maximize the demand that can be served, then the problem can be solved by the following mixed-integer-linear-program (MILP):

$$\begin{aligned} \max \quad & \sum_{i \in \mathcal{A}_r \cup \mathcal{A}_s} d_i \quad (4.42) \\ \text{s.t.} \quad & (4.40a)-(4.40b), (4.40c)-(4.40h), (4.41) \end{aligned}$$

Problem (4.42) is a simple approach to optimizing the number of vehicles that can be served. However, demand is typically origin-destination based in nature, so maximizing the total demand that is served may not be useful if travelers are not interested in those origin-destination proportions of travel.

### 4.3.2 Demand Maximization According to Origin to Destination Proportions under Limited Budget

Suppose that vehicular demand enters at the ratios of  $\hat{\mathbf{d}}$ . A natural objective is to serve as large a proportion of this demand as possible, i.e.  $\max \alpha$  where actual demand is  $\alpha \hat{\mathbf{d}}$ . Using equations (4.40a) and (4.40b), this demand can be distributed over links as

$$\alpha \hat{f}_i = \alpha \hat{d}_i \quad \forall i \in \mathcal{A}_r \cup \mathcal{A}_s \quad (4.43a)$$

$$\alpha \hat{f}_j = \alpha \sum_{i \in \mathcal{I}(j)} \hat{f}_i P_{ij} \quad \forall j \in \mathcal{A}_i \quad (4.43b)$$

with the amount of demand that can be served by limited deployment of max-pressure controls

$$\alpha_n \hat{f}_i P_{ij} \leq Q_{ij} \bar{S}_{ij} \quad \forall n \in \mathcal{N}, \forall (i, j) \in \mathcal{M}_n \quad (4.44)$$

This results in the following MILP:

$$\max \quad \alpha \quad (4.45a)$$

$$\text{s.t.} \quad \alpha \leq \alpha_n \quad \forall n \in \mathcal{N} \quad (4.45b)$$

$$\hat{f}_i = \hat{d}_i \quad \forall i \in \mathcal{A}_r \cup \mathcal{A}_s \quad (4.45c)$$

$$\hat{f}_j = \sum_{i \in \mathcal{I}(j)} \hat{f}_i P_{ij} \quad \forall j \in \mathcal{A}_i \quad (4.45d)$$

$$(4.40d)-(4.40h), (4.41), (4.44)$$

(4.45b) ensures that the system-wide  $\alpha$  is bounded by the lowest  $\alpha_n$ . So the maximization problem improves the lowest  $\alpha_n$  by installing MP control thus increasing system-wide  $\alpha$ . This constraint enables a greedy algorithm to solve this problem because we can just find the next lowest  $\alpha_n$  and if MP control is not installed there we can improve the system-wide  $\alpha$ . Since constraints (4.45c) and (4.45d) are independent of  $\alpha$ , they can be solved separately. Then, constraint (4.44) can be solved to find the maximum  $\alpha_n$  possible for each  $n$ . Because the overall system-wide  $\alpha$  is limited by the smallest  $\alpha_n$ , we present a decentralized greedy algorithm to solve the problem (4.45a). Algorithm 1 works by setting the signal capacity at each node initially equal to its current available capacity. Then, Algorithm 1 improves the node  $n'$  with active constraint (4.45b) until the maximum budget  $B$  is exhausted. Due to constraint (4.45b), improving any other node (although it may be more budget-efficient) would not yield an improvement on the overall  $\alpha$ .

**Theorem 4.** *If for a given budget,  $B$  the solution from the Algorithm 1 is  $\gamma'$  and a global optimal solution is  $\gamma^*$  then  $\gamma' = \gamma^*$ .*

*Proof.* By contradiction. Let  $\gamma'$  be the solution from the Algorithm 1 and let  $\gamma^*$  be a globally optimal solution with  $\alpha^* > \alpha'$ .

---

**Algorithm 1** Greedy algorithm to optimize max-pressure installations to find maximum  $\alpha$  ratio of served demand.

---

```

1: Solve eq. (4.45c) and eq. (4.45d) to obtain  $\hat{f}_i \forall i \in A_{all}$ 
2: for  $n \in N$  do
3:    $\bar{S}_n \leftarrow \tilde{S}_n$ 
4: end for
5: while  $B > 0$  do
6:    $n' \leftarrow \arg \min_{n \in N} \left\{ \max \left\{ \alpha_n : \alpha_n \hat{f}_i P_{ij} < Q_{ij} \bar{S}_n(i, j) \quad \forall (i, j) \in \mathcal{M}_n \right\} \right\}$ 
7:   if  $b_{n'} \leq B$  then
8:      $\bar{S}_{n'} \leftarrow \arg \max_{\hat{S}_{n'} \in \text{co}(\tilde{S}_{n'})} \left\{ \alpha_n : \alpha_n \hat{f}_i P_{ij} < Q_{ij} \hat{S}_{n'}(i, j) \quad \forall (i, j) \in \mathcal{M}_{n'} \right\}$ 
9:      $B \leftarrow B - b_{n'}$ 
10:  else
11:    break
12:  end if
13: end while

```

---

Case 1: Suppose that  $\gamma'_n = 1$  but  $\gamma_n^* = 0$ . Then,  $\alpha^* \leq \alpha_n$  by constraint (1), but  $\alpha_n \leq \alpha'$  because the Algorithm 1 selects nodes that lower bound  $\alpha'$  in line 6 of the Algorithm 1. Then,  $\alpha^* \leq \alpha_n \leq \alpha'$ , which contradicts  $\alpha^* > \alpha'$ .

Case 2: Suppose that  $\gamma'_n = 0$  but  $\gamma_n^* = 1$ . The Algorithm 1 terminates if budget is exhausted or less than the smallest MP installation cost according to line 5 and line 7 of Algorithm 1. So, at termination of the Algorithm 1, either all nodes use max pressure control or there is insufficient budget to improve  $\alpha$ . Therefore,  $\gamma' = \gamma^*$ .  $\square$

## 4.4 Numerical Results

To demonstrate the results we use the downtown Austin city network which was calibrated to match observed morning peak characteristics in 2011 by the Network Modelling Center at the University of Texas at Austin Levin et al. (2020). This network consists of 171 zones, 546 intersections, 150 signalized intersections and 1247 links. This network also includes most of the central business district of Austin, Texas. Arterials north of the city and the two major

north-south freeways are also included in this network. The network data also includes signal timings for the signalized intersections. All of the simulations used a timestep of 15 seconds and a total duration of 3 hours. All links were modeled using a point queue link model in simulation. Figure 4.1 shows the downtown Austin network with the MP control and signal control obtained from Austin network dataset shown by the red and green nodes respectively.

To obtain the turning proportion we ran Dynamic Traffic Assignment (DTA) using the Method of Successive Averages (MSA) algorithm. The DTA was run in a custom in-house simulator called AVDTA written in JAVA. The optimization problem Equation (4.45a) is then solved using the Algorithm 1 and these turning proportions to find the intersections where MP control should be installed. These MP control intersections are shown in Figure 4.1 by red nodes. To verify the accuracy of this result and to show the benefits of installing max pressure control on more nodes we ran simulations using AVDTA. We created simulations in AVDTA and determined the maximum stable demands using subsets of limited deployment nodes. From this point on the sum of the demands for the entry links will be referred to as the demand. So, the maximum stable demand would be the sum of the demands for all the entry links that can be stabilized. We also deployed MP in random nodes and determined the maximum stable demands for those MP installations. We then compared the maximum stable demands with limited deployment and random deployment of MP controller. We used the point queue link model in AVDTA because we used that model in our proof of stability.

First, 20 intersections selected by the optimization problem were chosen where MP control was implemented and in the other signalized intersections the original signal timings provided in the Austin network data were used. Denote this set of 20 nodes selected by the limited deployment nodes set by  $N_{ld}$ . We

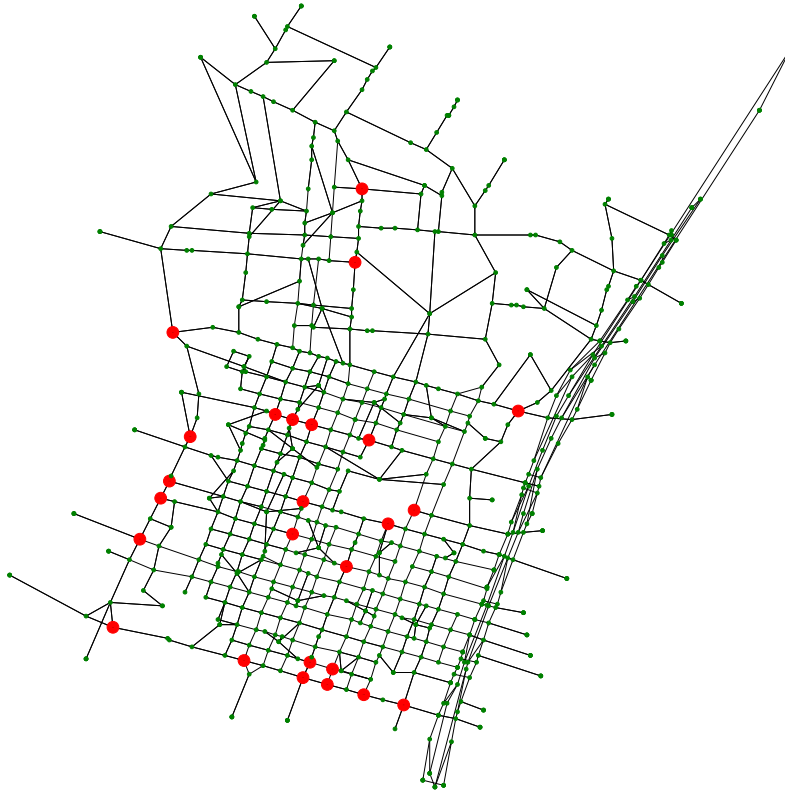


Figure 4.1: Downtown Austin network, red nodes are MP controlled and other nodes are controlled using timings from Austin network data.

also denote the sum of maximum stable demand by  $h_{|n|}$  for nodes  $n \subset N_{\text{Id}}$ . To find the  $h_{|n|}$  we formulate a decision problem: given some sum of demands for the entry links  $d$  and the AVDTA simulator as the verifier, can  $d$  be stabilized or is  $d \leq h_{|n|}$ ? We assume that any sum of demands  $d \leq h_{|n|}$  can be stabilized and  $d > d_{|n|}^s$  can not be stabilized. Using this assumption and the decision problem, we perform binary search for the maximum stable demands sum for  $n \subset N_{\text{Id}}$ . For a limited deployment of  $n \subset N_{\text{Id}}$  nodes where MP is installed, we define the stable demand sum  $h_{|n|}$  from the verifier AVDTA simulator as:  $h_{|n|}$  is stable if the best fitted line of the sum of queue lengths at time  $t$ , over the period starting from after a warmup period  $w$  to the end of simulation has a slope less than

some maximum predefined slope  $s \in \mathbb{R}_+$ . This definition ensures that the queue length will not grow to infinity with progression in time which is consistent with the formal definition of stability given in Definition 1. Similarly, we also find the maximum stable demands for random deployment of MP control.

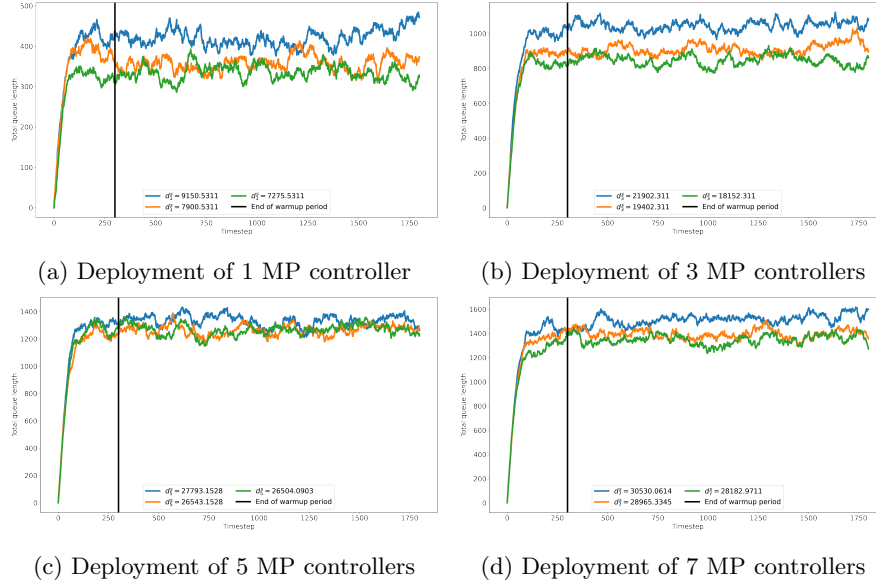


Figure 4.2: Stability detection by binary search for different deployments of MP control (Data from only 1 repetition of MC is plotted.)

We ran Monte Carlo (MC) simulations with 100 repetitions to decrease the effects of stochasticity while trying to find the stable demands. During our first run of the simulations we noticed that after about 200 timesteps the fluctuations in the queue length were not that large compared to before that warmup period. This is because during the first 200 timesteps there was plenty of space in the network for the vehicles to enter. After the 200 timesteps however, some vehicles needed to exit to make space for new vehicles to enter the network. To be safe we selected this warmup period to be 300 timesteps for all the simulations. The large change in queue length before the 200 timesteps can be seen in the Figure 4.2. For the maximum slope  $s$  of the fitted line we tested

several values which are plotted in Figure 4.3. The maximum slope needed to be very small to ensure that the fitted straight line is close to horizontal which would indicate stability. However, a slight positive slope is allowable since over a period of 3 hours if the total average queue length increases by 1 – 5 vehicles then the demand can still be reasonably considered to be stable. We used two slopes, 0.0001 and 0.0005 which approximately translates to an increase of 1 and 5 vehicles over the 3 hour simulation period respectively. Manual human inspection of the stability plots can be done to detect stability with higher accuracy. However, to ensure reproducibility of results we avoided manual human inspection to determine stability and used the maximum slopes. Further research should address this issue of stability detection. For a split of 0.50 if at least 50% repetitions of a simulation for a demand was stable then that demand was considered to be stabilizable otherwise unstabilizable. Since detection of stability is very sensitive, we also used a split of 0.40. Therefore, if a demand was identified to be stable for 40% of the MC repetitions then that demand would be considered stable.

The theoretical stable demand sum for limited deployment of  $n$  nodes line in Figure 4.3 shows that after installing MP in 7 nodes, more MP installations did not result in significant increase in maximum stable demand. This is because the system wide  $\alpha$  is lower bounded by the minimum  $\alpha_n$ . Therefore, even if installation of MP control results in increase of  $\alpha_n$  in node  $n$  it will not increase the system wide  $\alpha$  if another node  $n'$  where MP is already installed has  $\alpha_{n'} = \alpha$  and  $\alpha_{n'} < \alpha_n$ . This means even though installing MP in a node may increase its performance in terms of throughput, the maximum stable demand may still be bounded. With different choice of parameters the stability detection method caused the binary search to converge to different maximum stable demands as shown in Figure 4.3. The pattern in which the maximum stable demand changed

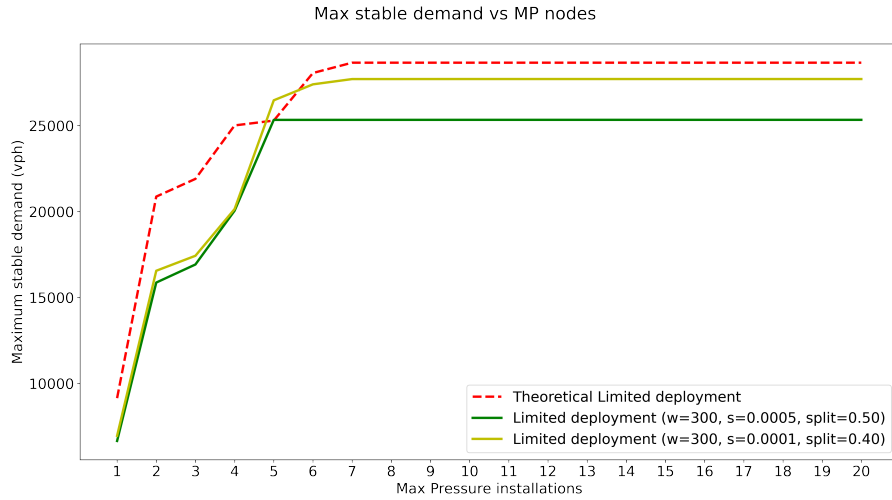


Figure 4.3: Maximum stable demands achieved with different deployment policies of MP nodes.

however was mostly similar to theoretical results. With a warmup, maximum slope and split of 300 timesteps, 0.0005, 0.50 respectively, the trend of increase in maximum stable demand followed theoretical results except for the change from 4 to 5 deployed nodes. Figure 4.3 shows that theoretical limited deployment predicted a much flatter increase where simulation determined a much steeper increase in the maximum stable demand. The optimization problem considers average signal timing for MP control and but the simulation was only repeated a limited number of times and also the stability detection method not being perfect may explain this discrepancy.

Then, we selected random nodes to install MP control and then determined the maximum stable demand using the same method. Figure 4.4 shows the maximum stable demands for both limited and random deployment of MP controlled nodes. For the random deployment, the same stability detection parameters were used. Figure 4.4 shows that with the same stability detection parameters limited deployment was able to stabilize more demand than random

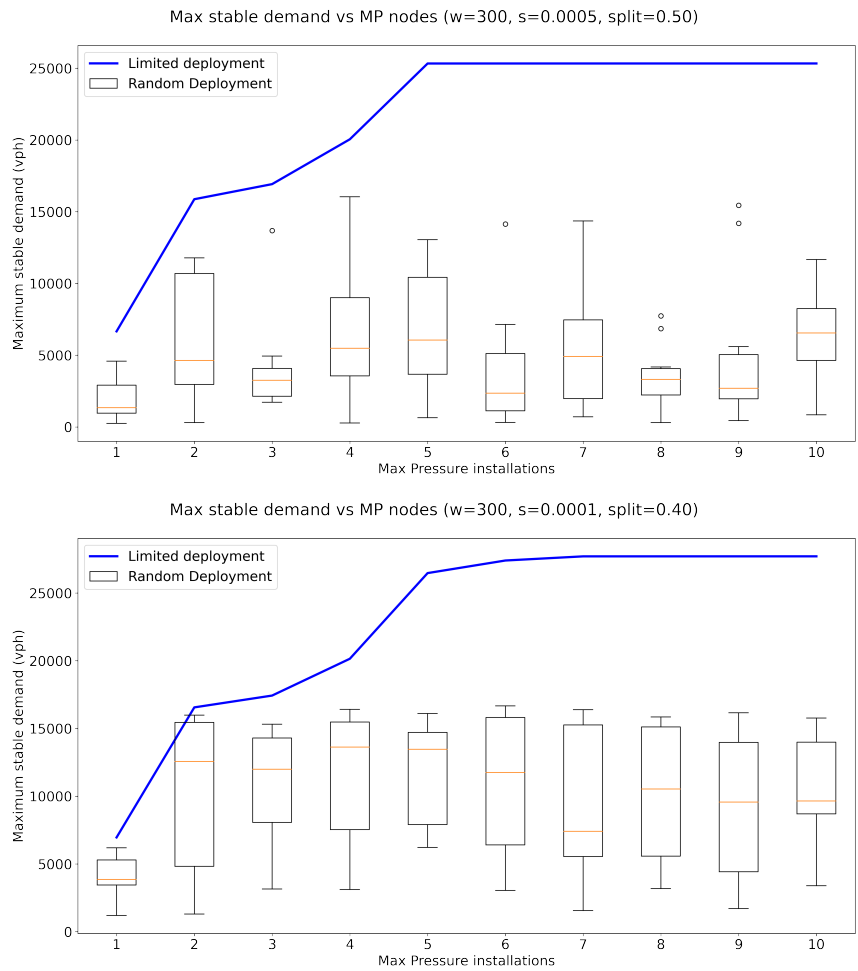
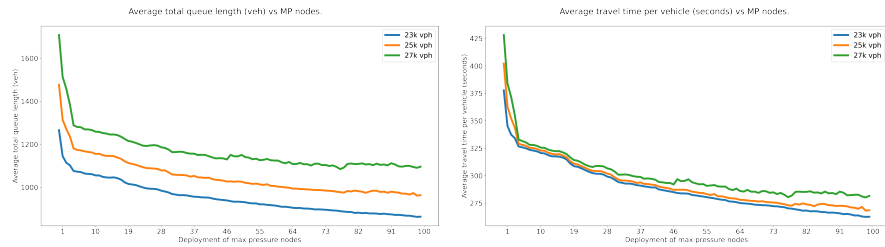


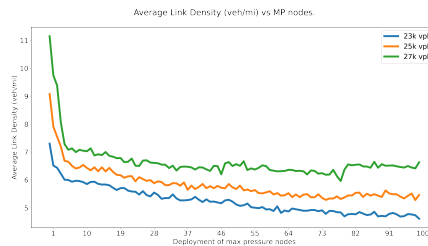
Figure 4.4: Maximum stable demands achieved with different deployment policies of MP nodes.

deployment. So, even though stability detection is not perfect using the same parameters for stability detection, limited deployment performed better than random deployment to increase system performance.

The maximum stable demand bound does not mean installing max pressure control in more nodes will not result in more benefits. We used Monte Carlo simulations with 10 repetitions to demonstrate the impacts of limited deployment of up to 100 nodes on different aspects of network performance. We ran these simulations with a fixed number of vehicles inserted per hour into the network. The other parameters of the simulations were kept unchanged.



(a) Average total queue length with increase in limited deployment. (b) Average travel time per vehicle with increase in limited deployment.



(c) Average link density with increase in limited deployment.

Figure 4.5: Change in different performance metrics with increase in limited deployment.

Figure 4.5 shows decreasing trends in total average queue length, average travel times and link densities as deployment of MP control increases. For higher demand even installing MP control in a few intersections yielded better performance which is consistent with our theory. Figure 4.3 shows that deploy-

ment of MP control resulted in high increase in maximum stable demand in the beginning but after a certain number of installations the maximum stable demand could not be increased anymore. Figure 4.5 shows a similar pattern. Since the maximum stable demand becomes bounded after a certain number of MP control installations the performance benefits resulting from more MP control deployment do not increase as much anymore. However, a small increase in benefits with more MP controllers is still noticeable from the Figure 4.5. In particular, the decrease in average travel time per vehicle demonstrates how limited deployment of MP controllers benefit the system performance. These results indicate that as the deployment of MP control increases the system performance also increases. System performance depends on the maximum stabilizable demands which is also shown to increase with limited deployment.



# Chapter 5

## Conclusions

### 5.1 Performance Evaluation of Modified Cyclic MP in Simulation

Chapter 3 showed that the max-pressure controllers outperformed current AC controllers in most of the intersections under various demands in terms of delays. Using the best parameters for delay reduction, the MP controllers managed to increase throughput compared to the current AC signal controllers in most intersections. CMP-S was able to reduce the worst lane's total delay in most intersections under various demand periods. The frequent change of phases corroborates that the MP controllers were indeed reacting to real-time traffic and other performance metrics reveal that this reaction was positive in most cases. The phase changed most frequently using CMP-S followed by CMP-NS, AMP and AC controllers in that order.

Running simulations with different sets of parameters and selecting the set for which the highest performance was achieved seems to be a way to select the set of best parameters. This thesis provides some insight on how to reduce the

number of the parameters that should be tested. AMP control performed best with smaller MP timesteps for most of the intersections during the different demand periods in terms of delay reduction. However, during some peak periods at some intersections higher MP timesteps performed the best. For the CMP-S control, in some cases different combinations of MP timestep and max cycle length performed best while in other cases only a specific combination of those two parameters performed best. Inadequate maximum cycle length to activate all phases at least for the duration of MP timestep reduces performance. After ensuring maximum cycle length is high enough to accommodate the activation of all phases increasing maximum cycle length up to a certain point increased performance. Increasing maximum cycle length beyond that value did not increase performance anymore. Very high maximum cycle length also can cause decrease in performance if a sub-optimal phase is activated repeatedly due to inaccurate pressure approximation especially in shared lanes and where high asymmetric traffic is observed. It is still not completely clear how the parameters affect performance. More experiments with a variety of intersection geometries and traffic demand should be conducted.

Even though the CMP controllers perform worse than AMP controller the cyclicity of phase change is preferred for implementation in real roads. CMP controllers were able to reduce delays in most cases compared to the AC signal controllers. During the peak periods CMP-NS performed slightly worse because it had to activate each phase at least once which resulted in some wastage of green time when no vehicles were present. CMP-S solved this problem by modifying the CMP-NS formulation to have the ability to skip phases which increased green time utilization. CMP-S outperformed the AC controllers under almost all demands at different intersections based on several metrics.

The MP controllers performed slightly worse in terms of throughput maxi-

mization at the intersections with more shared lanes during high traffic demand periods. Assumption of point queue with infinite link capacity may have limited the performance during the heavy demand periods. Also, not considering first-in-first-out (FIFO) traffic behavior left AMP open to the possibility of gridlocks due to low volume of blocking traffic in front of the traffic queue. CMP-NS and CMP-S solves this issue to some extent, however inclusion of FIFO traffic behavior in the formulation should increase performance even more at the intersections with shared lanes.

## 5.2 Throughput Properties and Optimal Intersections

Chapter 4 discussed the problem of deployment of MP controllers under limited budget. Previous studies proved that the MP controller is throughput maximizing with the condition that all of the signalized intersections use MP control. However, installing MP control in all intersections may not be possible considering budget limitations. Therefore, this thesis analyzed whether MP control can still guarantee maximum throughput with limited deployment. We showed that even with limited deployment MP control can still achieve maximum throughput, but with less MP controlled intersections the stable region is smaller. Then, we presented a MILP to find the optimal intersections to install MP control. We designed a greedy algorithm to solve the MILP efficiently and proved that it can solve the problem to optimality. Using that problem we determined the theoretical maximum stable demands for deployment of MP controllers under different budgets. We presented how maximum stable demand from simulations can be determined using a search algorithm using a decision problem and the simulator. Then, we ran simulations with Monte Carlo repetitions in AVDTA,

our custom simulator to verify the theoretical results. After analyzing the downtown Austin network, we found that after installing MP control in only a few intersections most of the maximum stabilizable demand from standard MP control could be served. We then compared and showed how the theoretical results mostly matched with the results from the simulator. We also ran simulations with fixed demands and increasing number of MP control deployments to see its effect on system performance. The decrease in average queue length and link density shows the network benefits and the decrease in average travel time per vehicle shows how limited deployment benefits the travellers. We found that installing more MP controllers after reaching the maximum stabilizable demand further increased the system performance. Therefore, installing more MP controllers is desirable.

### 5.3 Limitations and Recommendations

The max-pressure controls implemented in simulation in this thesis do not consider the capacity of the downstream link like Gregoire et al. (2014b) to normalize queue lengths. Gregoire et al. (2014b) and Sun and Yin (2018) showed that MP with such normalized queue lengths are an improvement over Varaiya (2013)'s max-pressure control. How CMP controllers perform with normalized queues with adaptive routing should be an interesting study. We approximated the next turn or movement of vehicles based on the lanes the vehicles were occupying using data from the loop detectors setup in simulation. However, vehicles may not always enter the correct lane to make their movement through the intersection which is not considered during queue length calculation in this thesis. This thesis also does not consider FIFO traffic behavior for the max-pressure controllers and we intend to address that in future studies. We are also planning to conduct real life experiments with max-pressure controllers in the future.

In this thesis, we assumed the point queue link model which does not describe the traffic conditions perfectly. Future work should focus on analyzing the stability properties and conducting simulations with a more realistic link model. More networks with different network geometries should be analyzed numerically. Combinations of deployment of MP controller and multiple other controllers should also be studied to see if system performance can be improved. Considering pedestrian traffic and explicit signal coordination between intersections with same or different types of controllers should be interesting to study. How different levels of market penetration of CAV's would affect limited deployment of MP control should also be an interesting and realistic problem to consider. Since MP control relies heavily on sensors to detect queue lengths it can be vulnerable to cyber attacks. Methods of detecting such attacks and designing fail-safe controls should also be studied.



# Bibliography

Jennie Lioris, Alex Kurzhanskiy, and Pravin Varaiya. Adaptive max pressure control of network of signalized intersections. *IFAC-PapersOnLine*, 49(22): 19–24, 2016a.

Michael W. Levin and S. Boyles. Pressure-based policies for reservation-based intersection control. In *96th Annual Meeting of the Transportation Research Board, Washington, DC.*, 2017.

Xiaotong Sun and Yafeng Yin. A simulation study on max pressure control of signalized intersections. *Transportation Research Record*, 2672(18):117–127, 2018.

Pravin Varaiya. Max pressure control of a network of signalized intersections. *Transportation Research Part C: Emerging Technologies*, 36:177–195, 2013.

Tichakorn Wongpiromsarn, Tawit Uthaicharoenpong, Yu Wang, Emilio Frazzoli, and Danwei Wang. Distributed traffic signal control for maximum network throughput. In *2012 15th International IEEE Conference on Intelligent Transportation Systems*, pages 588–595, 2012. doi: 10.1109/ITSC.2012.6338817.

Nan Xiao, Emilio Frazzoli, Yitong Li, Yu Wang, and Danwei Wang. Pressure

- releasing policy in traffic signal control with finite queue capacities. In *53rd IEEE Conference on Decision and Control*, pages 6492–6497. IEEE, 2014.
- William S. Vickrey. Pricing in urban and suburban transport. *The American Economic Review*, 53(2):452–465, 1963. ISSN 00028282. URL <http://www.jstor.org/stable/1823886>.
- H. M. Zhang, Yu (Marco) Nie, and Zhen (Sean) Qian. Modelling network flow with and without link interactions: the cases of point queue, spatial queue and cell transmission model. *Transportmetrica B: Transport Dynamics*, 1(1): 33–51, 2013. doi: 10.1080/21680566.2013.785921. URL <https://doi.org/10.1080/21680566.2013.785921>.
- C. Gawron. An iterative algorithm to determine the dynamic user equilibrium in a traffic simulation model. *International Journal of Modern Physics C*, 09(03):393–407, 1998. doi: 10.1142/S0129183198000303. URL <https://doi.org/10.1142/S0129183198000303>.
- Tung Le, Péter Kovács, Neil Walton, Hai L Vu, Lachlan LH Andrew, and Serge SP Hoogendoorn. Decentralized signal control for urban road networks. *Transportation Research Part C: Emerging Technologies*, 58:431–450, 2015.
- Michael W. Levin, Jeffrey Hu, and Michael Odell. Max-pressure signal control with cyclical phase structure. *Transportation Research Part C: Emerging Technologies*, 120:102828, 2020. ISSN 0968-090X. doi: <https://doi.org/10.1016/j.trc.2020.102828>. URL <https://www.sciencedirect.com/science/article/pii/S0968090X20307324>.
- Simanta Barman and Michael W. Levin. Performance evaluation of modified cyclic max-pressure controlled intersections in realistic corridors. *Transportation Research Record*, 0(0):03611981211072807, 2022. doi: 10.1177/03611981211072807. URL <https://doi.org/10.1177/03611981211072807>.

- L. Tassiulas and A. Ephremides. Stability properties of constrained queueing systems and scheduling policies for maximum throughput in multihop radio networks. *IEEE Transactions on Automatic Control*, 37(12):1936–1948, 1992. doi: 10.1109/9.182479.
- Jean Gregoire, Emilio Frazzoli, Arnaud de La Fortelle, and Tichakorn Wongpiromsarn. Back-pressure traffic signal control with unknown routing rates. *CoRR*, abs/1401.3357, 2014a. URL <http://arxiv.org/abs/1401.3357>.
- Jean Gregoire, Xiangjun Qian, Emilio Frazzoli, Arnaud De La Fortelle, and Tichakorn Wongpiromsarn. Capacity-aware backpressure traffic signal control. *IEEE Transactions on Control of Network Systems*, 2(2):164–173, 2014b.
- Rui Sha and Andy HF Chow. A comparative study of centralised and decentralised architectures for network traffic control. *Transportation Planning and Technology*, 42(5):459–469, 2019.
- Nan Xiao, Emilio Frazzoli, Yiwen Luo, Yitong Li, Yu Wang, and Danwei Wang. Throughput optimality of extended back-pressure traffic signal control algorithm. In *2015 23rd Mediterranean Conference on Control and Automation (MED)*, pages 1059–1064, 2015a. doi: 10.1109/MED.2015.7158897.
- Nan Xiao, Emilio Frazzoli, Yitong Li, Yiwen Luo, Yu Wang, and Danwei Wang. Further study on extended back-pressure traffic signal control algorithm. In *2015 54th IEEE Conference on Decision and Control (CDC)*, pages 2169–2174, 2015b. doi: 10.1109/CDC.2015.7402528.
- Jian Wu, Dipak Ghosal, Michael Zhang, and Chen-Nee Chuah. Delay-based traffic signal control for throughput optimality and fairness at an isolated intersection. *IEEE Transactions on Vehicular Technology*, 67(2):896–909, 2018. doi: 10.1109/TVT.2017.2760820.

- Li Li and Saif Eddin Jabari. Position weighted backpressure intersection control for urban networks. *Transportation Research Part B: Methodological*, 128: 435–461, 2019.
- ShenXue Hao and LiCai Yang. Traffic network modeling and extended max-pressure traffic control strategy based on granular computing theory. *Mathematical Problems in Engineering*, 2019, 2019.
- Jennie Lioris, Alex Kurzhanskiy, and Pravin Varaiya. Adaptive max pressure control of network of signalized intersections. *IFAC-PapersOnLine*, 49 (22):19–24, 2016b. ISSN 2405-8963. doi: <https://doi.org/10.1016/j.ifacol.2016.10.366>. URL <https://www.sciencedirect.com/science/article/pii/S240589631631953X>. 6th IFAC Workshop on Distributed Estimation and Control in Networked Systems NECSYS 2016.
- Anastasios Kouvelas, Jennie Lioris, S. Alireza Fayazi, and Pravin Varaiya. Maximum pressure controller for stabilizing queues in signalized arterial networks. *Transportation Research Record*, 2421(1):133–141, 2014. doi: [10.3141/2421-15](https://doi.org/10.3141/2421-15). URL <https://doi.org/10.3141/2421-15>.
- SA Ramadhan, HY Sutarto, GS Kuswana, and E Joelianto. Application of area traffic control using the max-pressure algorithm. *Transportation planning and technology*, 43(8):783–802, 2020.
- Wanli Chang, Debayan Roy, Shuai Zhao, Anuradha Annaswamy, and Samarjit Chakraborty. Cps-oriented modeling and control of traffic signals using adaptive back pressure. In *2020 Design, Automation & Test in Europe Conference & Exhibition (DATE)*, pages 1686–1691. IEEE, 2020.
- Hao Yu, Pan Liu, Yueyue Fan, and Guohui Zhang. Developing a decentralized signal control strategy considering link storage capacity. *Transportation Research Part C: Emerging Technologies*, 124:102971, 2021.

- Michael J Smith, Takamasa Iryo, Richard Mounce, Marco Rinaldi, and Francesco Viti. Traffic control which maximises network throughput: Some simple examples. *Transportation Research Part C: Emerging Technologies*, 107:211–228, 2019.
- Pedro Mercader, Wasim Uwayid, and Jack Haddad. Max-pressure traffic controller based on travel times: An experimental analysis. *Transportation Research Part C: Emerging Technologies*, 110:275–290, 2020.
- Vinayak Dixit, Divya Jayakumar Nair, Sai Chand, and Michael W Levin. A simple crowdsourced delay-based traffic signal control. *PLoS one*, 15(4):e0230598, 2020.
- Li Li, Victor Okoth, and Saif Eddin Jabari. Backpressure control with estimated queue lengths for urban network traffic. *IET Intelligent Transport Systems*, 15(2):320–330, Jan 2021a. ISSN 1751-9578. doi: 10.1049/itr2.12027. URL <http://dx.doi.org/10.1049/itr2.12027>.
- Rongsheng Chen, Jeffrey Hu, Michael W Levin, and David Rey. Stability-based analysis of autonomous intersection management with pedestrians. *Transportation Research Part C: Emerging Technologies*, 114:463–483, 2020.
- Michael W Levin, David Rey, and Adam Schwartz. Max-pressure control of dynamic lane reversal and autonomous intersection management. *Transportmetrica B: Transport Dynamics*, 7(1):1693–1718, 2019.
- David Rey and Michael W Levin. Blue phase: Optimal network traffic control for legacy and autonomous vehicles. *Transportation Research Part B: Methodological*, 130:105–129, 2019.
- Chia-Cheng Yen, Dipak Ghosal, Michael Zhang, Chen-Nee Chuah, and Hao Chen. Falsified data attack on backpressure-based traffic signal control algo-

rithms. In *2018 IEEE Vehicular Networking Conference (VNC)*, pages 1–8, 2018. doi: 10.1109/VNC.2018.8628334.

Thomas Pumir, Leah Anderson, Dimitrios Triantafyllos, and Alexandre M Bayen. Stability of modified max pressure controller with application to signalized traffic networks. In *2015 American Control Conference (ACC)*, pages 1879–1886. IEEE, 2015.

Leah Anderson, Thomas Pumir, Dimitrios Triantafyllos, and Alexandre M Bayen. Stability and implementation of a cycle-based max pressure controller for signalized traffic networks. *Networks & Heterogeneous Media*, 13(2):241, 2018.

Jingnan Cao, Yonghui Hu, Manolis Diamantis, Siyu Zhang, Yibing Wang, Jingqiu Guo, Ioannis Papamichail, Markos Papageorgiou, Lihui Zhang, and Jun Simon Hu. A max pressure approach to urban network signal control with queue estimation using connected vehicle data. In *2020 IEEE 23rd International Conference on Intelligent Transportation Systems (ITSC)*, pages 1–8. IEEE, 2020.

Siyu Zhang, Manolis Diamantis, Yibing Wang, Jingqiu Guo, Ioannis Papamichail, Markos Papageorgiou, Lihui Zhang, and Jun Simon Hu. Joint queue estimation and max pressure control for signalized urban networks with connected vehicles. In *2020 Forum on Integrated and Sustainable Transportation Systems (FISTS)*, pages 211–217. IEEE, 2020.

Henk Taale, Joost van Kampen, and Serge Hoogendoorn. Integrated signal control and route guidance based on back-pressure principles. *Transportation Research Procedia*, 10:226–235, 2015.

Jean Gregoire, Samitha Samaranyake, and Emilio Frazzoli. Back-pressure traf-

fic signal control with partial routing control. In *2016 IEEE 55th Conference on Decision and Control (CDC)*, pages 6753–6758. IEEE, 2016.

Ying Liu, Juntao Gao, and Minoru Ito. Back-pressure based adaptive traffic signal control and vehicle routing with real-time control information update. In *2018 IEEE International Conference on Vehicular Electronics and Safety (ICVES)*, pages 1–6. IEEE, 2018.

Te Xu, Simanta Barman, Michael W Levin, Rongsheng Chen, and Tianyi Li. Integrating public transit signal priority into max-pressure signal control: Methodology and simulation study on a downtown network. *Transportation Research Part C: Emerging Technologies*, 138:103614, 2022.

Li Li, Theodoros Pantelidis, Joseph YJ Chow, and Saif Eddin Jabari. A real-time dispatching strategy for shared automated electric vehicles with performance guarantees. *Transportation Research Part E: Logistics and Transportation Review*, 152:102392, 2021b.

Di Kang and Michael W Levin. Maximum-stability dispatch policy for shared autonomous vehicles. *Transportation Research Part B: Methodological*, 148:132–151, 2021.

Te Xu, Michael W. Levin, and Maria Cieniawski. A zone-based dynamic queuing model and maximum-stability dispatch policy for shared autonomous vehicles. In *2021 IEEE International Intelligent Transportation Systems Conference (ITSC)*, pages 3827–3832, 2021. doi: 10.1109/ITSC48978.2021.9565127.

Pablo Alvarez Lopez, Michael Behrisch, Laura Bieker-Walz, Jakob Erdmann, Yun-Pang Flötteröd, Robert Hilbrich, Leonhard Lücken, Johannes Rummel, Peter Wagner, and Evamarie Wießner. Microscopic traffic simulation using sumo. In *The 21st IEEE International Conference on Intelligent Transportation Systems*. IEEE, 2018. URL <https://elib.dlr.de/124092/>.

A. J. Hoffman and J. B. Kruskal. *13. Integral Boundary Points of Convex Polyhedra*, pages 223–246. Princeton University Press, 2016. doi: doi:10.1515/9781400881987-014. URL <https://doi.org/10.1515/9781400881987-014>.

Edwin KP Chong and Stanislaw H Zak. *An introduction to optimization*. John Wiley & Sons, 2004.